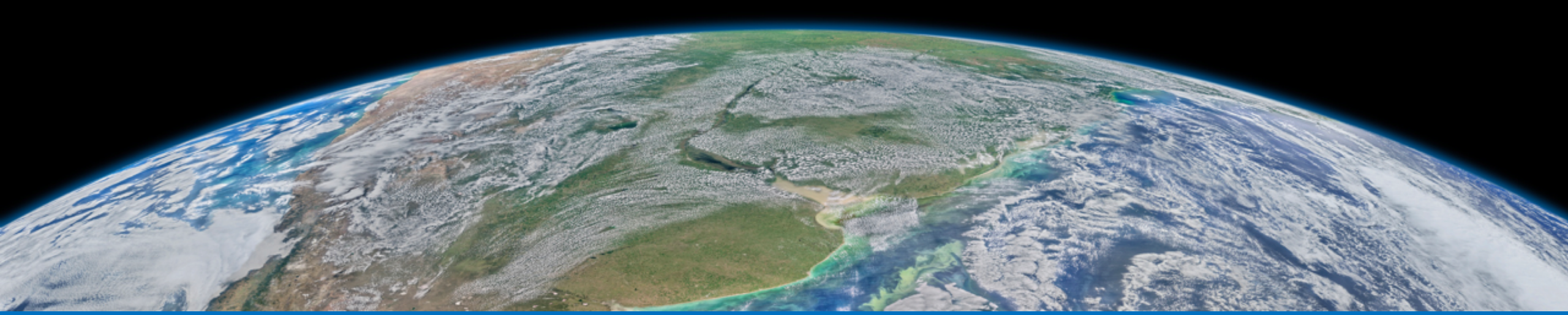


Mapping of phytoplankton functional types from hyperspectral images in Long Island Sound



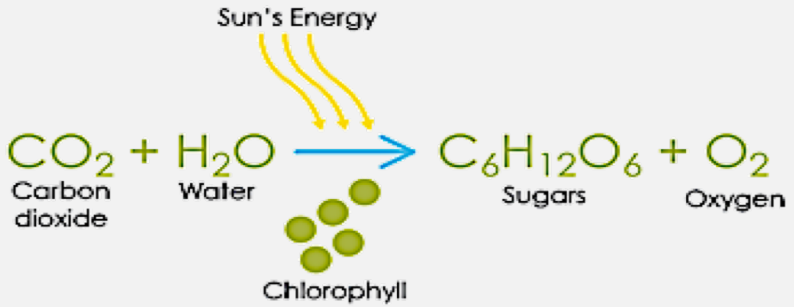
Jinghui Wu, Joaquim I. Goes, , Helga do. R. Gomes
Lamont Doherty Earth Observatory at Columbia University, New York, USA

Phytoplankton and blooms

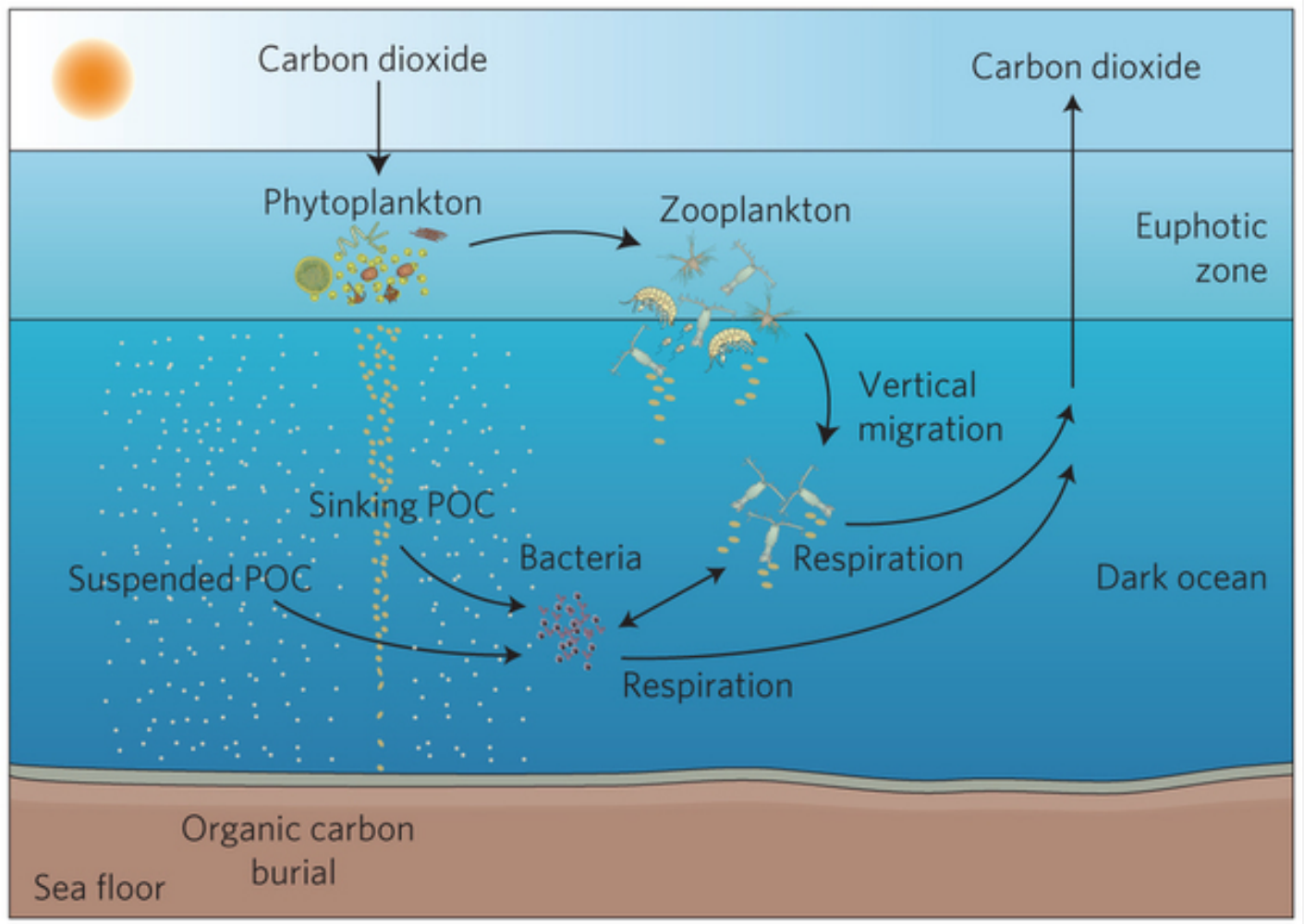
Phytoplankton

Photosynthesis | Primary Production

Pigments



Ocean carbon cycle



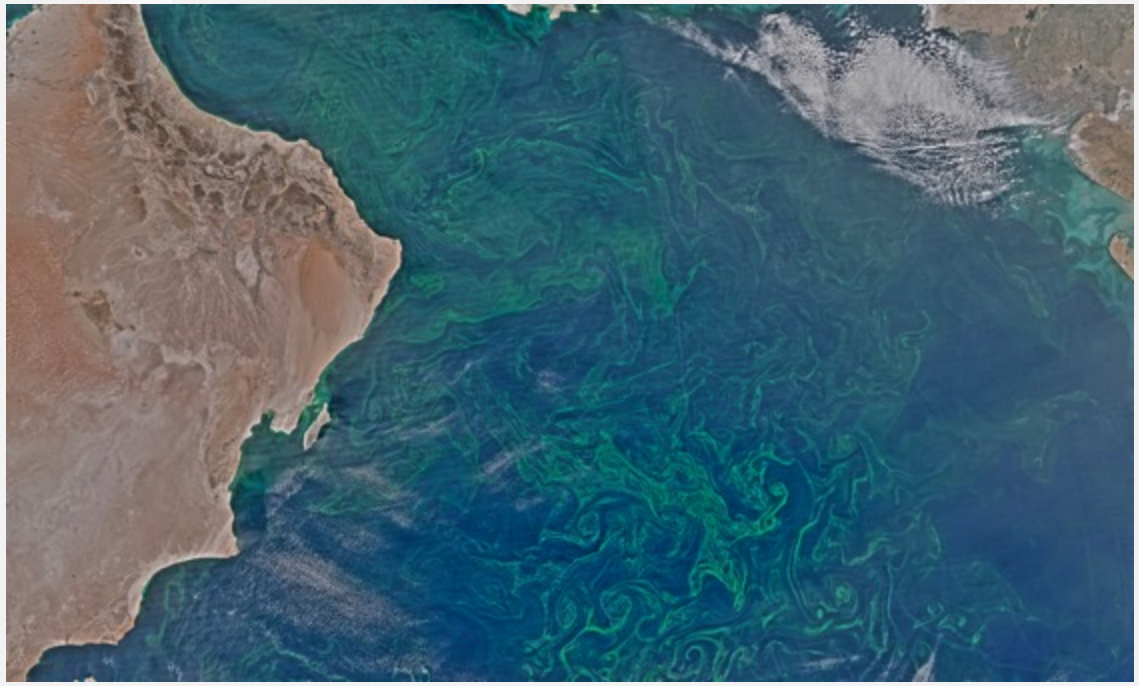


Phytoplankton boasts an amazing variety of forms and species. (Illustration: www.secchidisk.org)

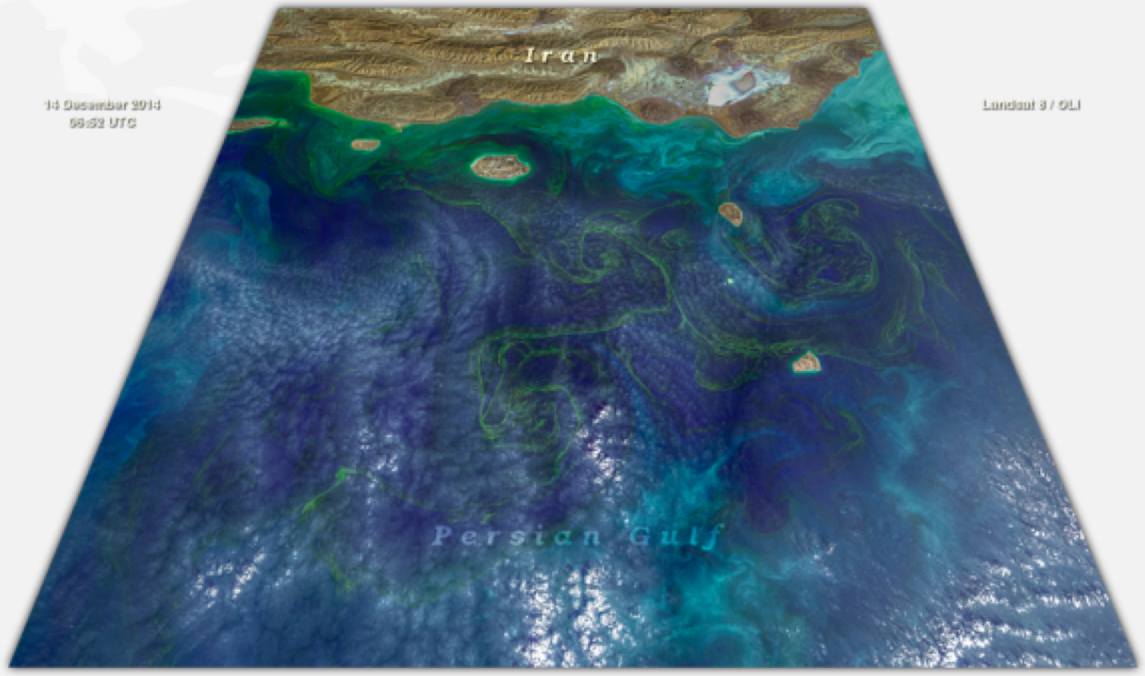
Phytoplankton and blooms

Arabian Sea Winter Blooms

Filamentous green swirls fill the northern Arabian Sea in February 2015 by Aqua MODIS.



This view of the southeastern end of the Persian Gulf was collected by Landsat 8 on December 14, 2018.



Dinoflagellate Bloom

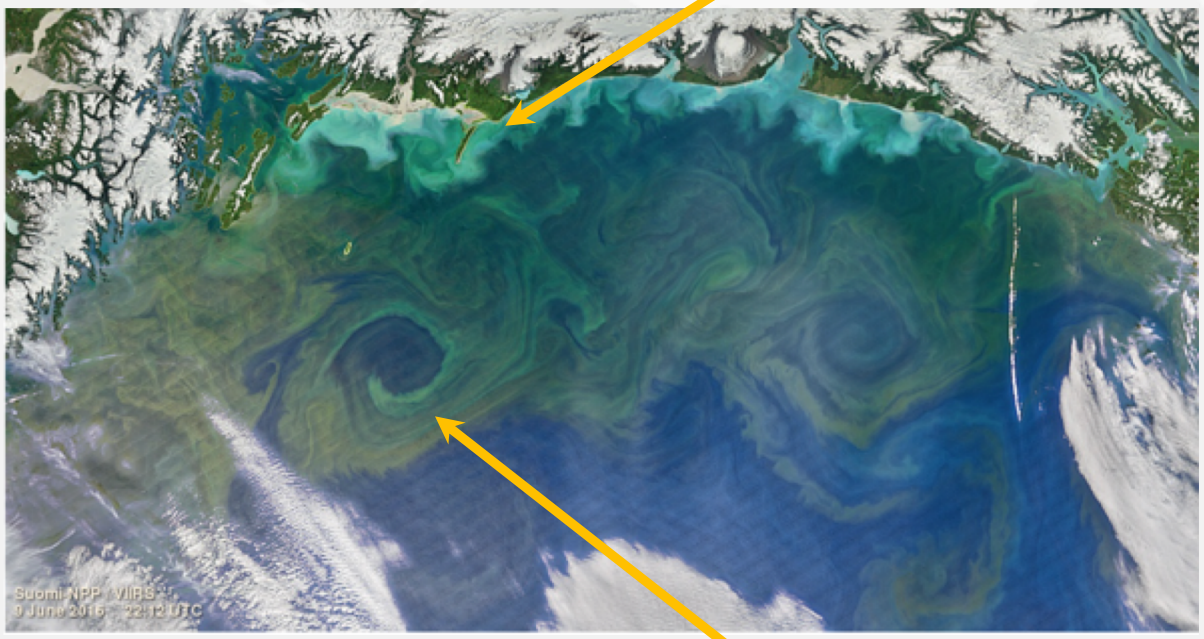
(Noctiluca scintillans)

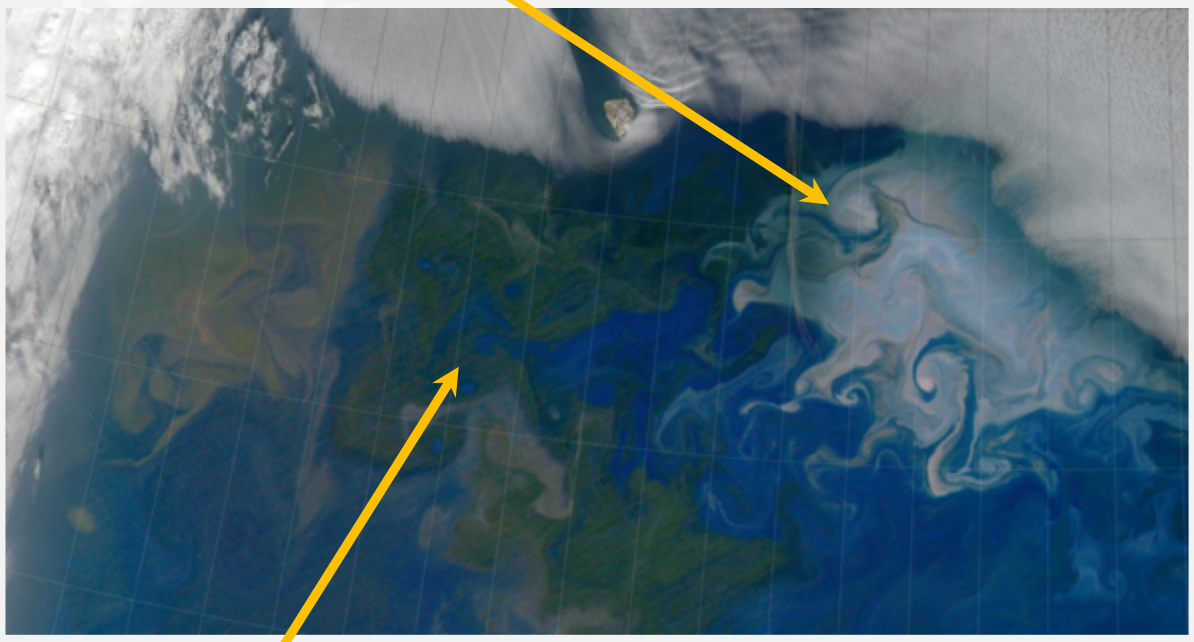
Phytoplankton and blooms

Barents Sea Blooms

Recent work suggests that diatoms predominate during May in the Barents Sea while coccolithophores bloom in August.

Coccolithophore Bloom



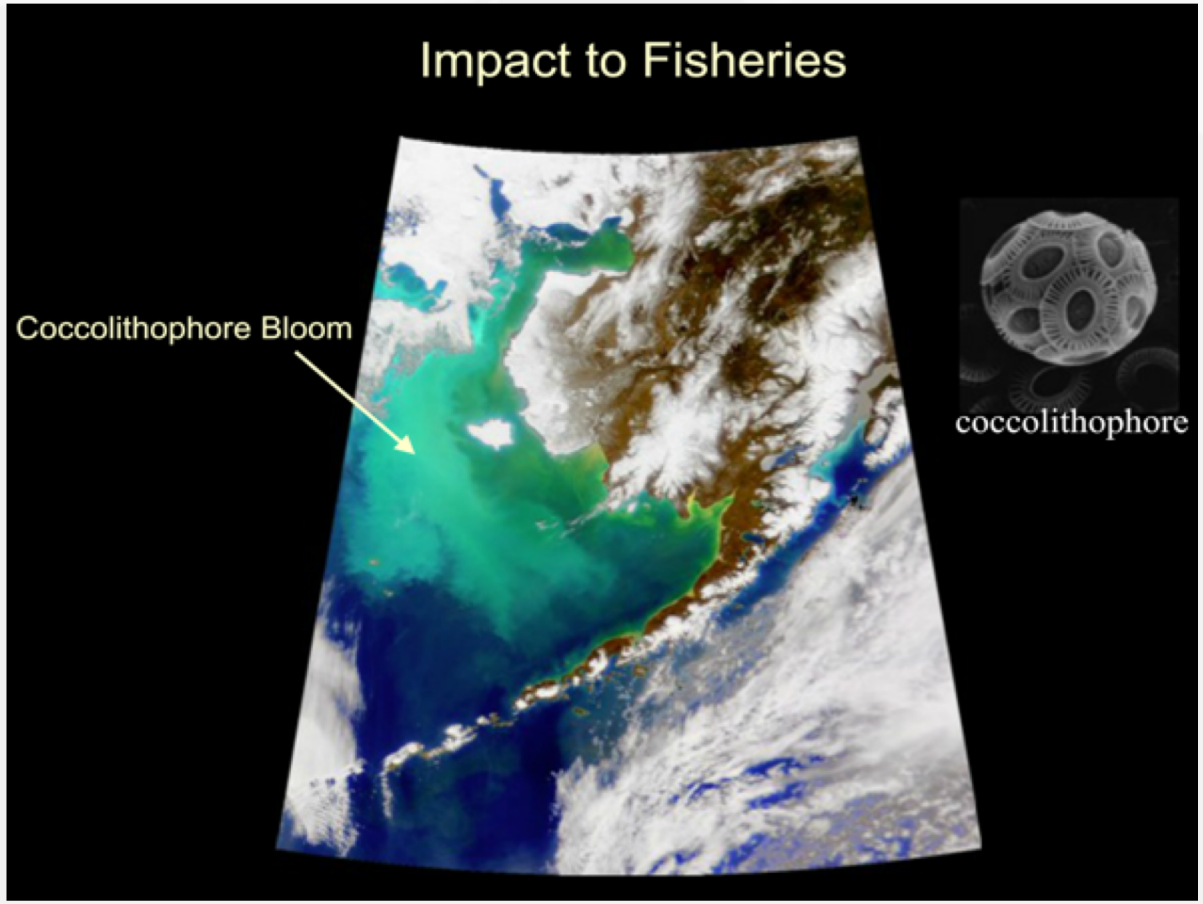


Diatom Bloom

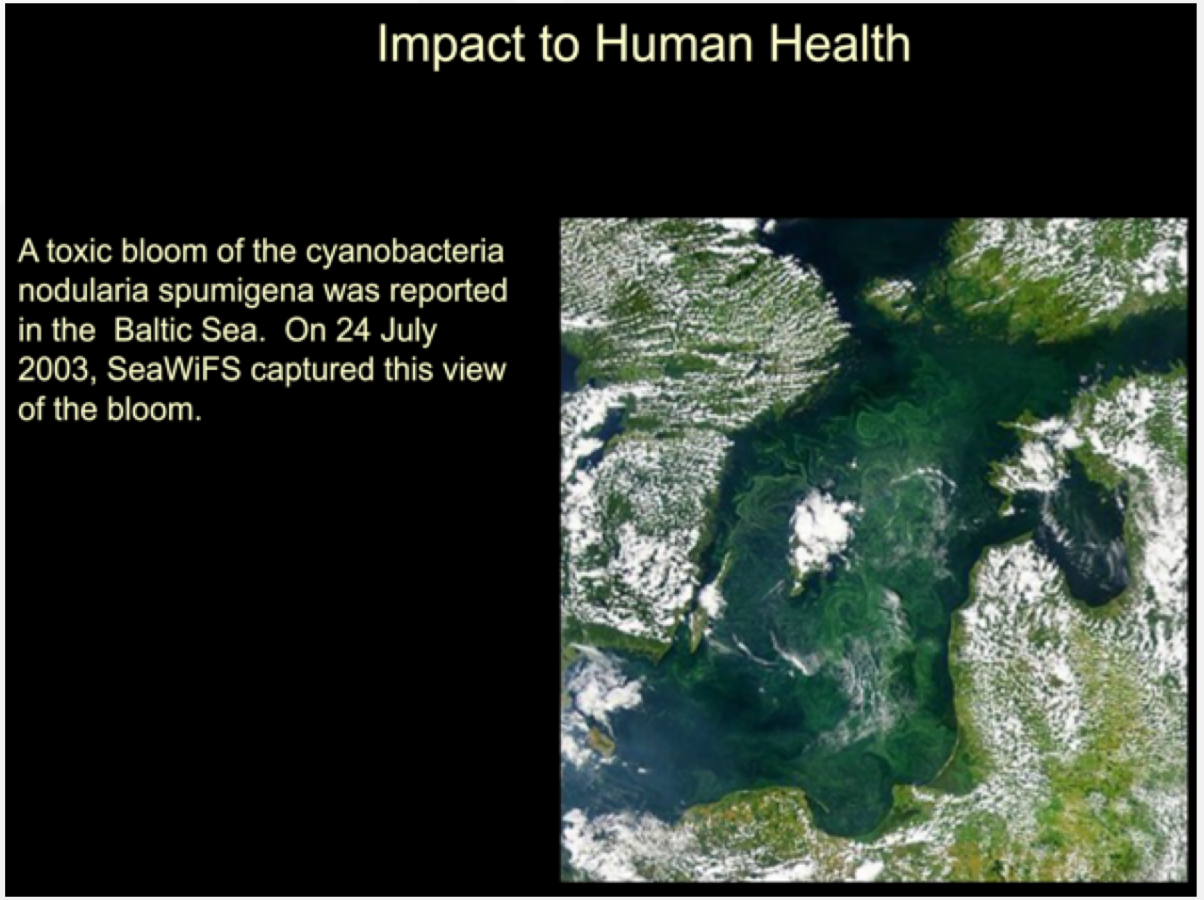
This view of the Gulf of Alaska was collected by VIIRS on June 9th, 2016.

This view was collected by Aqua-MODIS on July 14th, 2014.

Phytoplankton and blooms



Coccolithophore Bloom



Cyanobacteria Bloom

Phytoplankton and blooms

- Marine Protected Areas
- Marine Fisheries
- Animal Migrations
- Water Quality
- **Harmful Algal Blooms (HABs)**
- Eutrophication
- Coral Reef Health
- Marsh Subsidence
- Coastal Development



Red Tide

Phytoplankton Function Types (PFTs)

Diatoms



Pigments:

- chlorophyll (*a* and *c*)
- carotenoids (fucoxanthin)
- xanthophylls

Color:

yellowish-brown to olive-brown

Cyanobacteria



Pigments:

- phycobilisomes
- chlorophyll a
- chlorophyll b

Color:

blue-green

Dinoflagellate



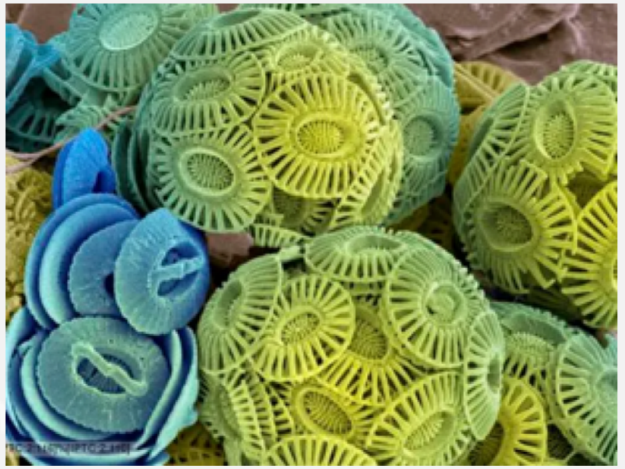
Pigments:

- chlorophyll *a*, c2
- Xanthophylls
- carotenoids

Color:

golden brown

Coccolithophores



Pigments:

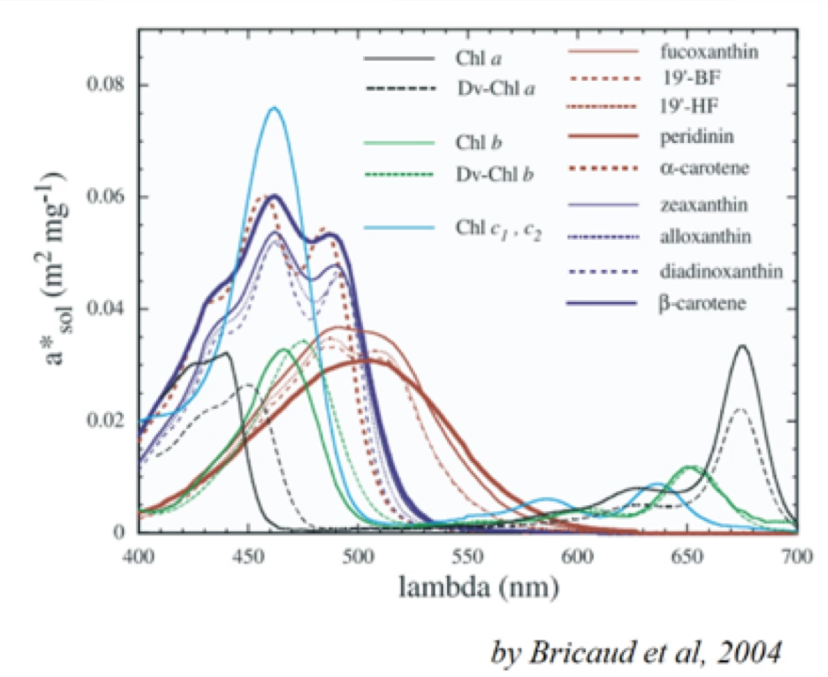
- chlorophyll *a*, c_s
- Fucoxanthin derivatives

Color:

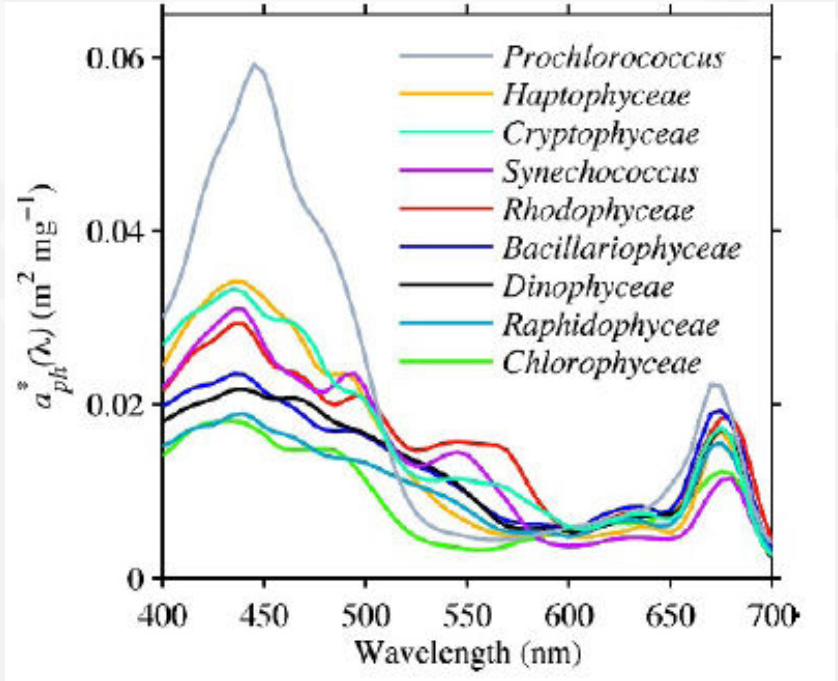
milky blue

Phytoplankton Pigments

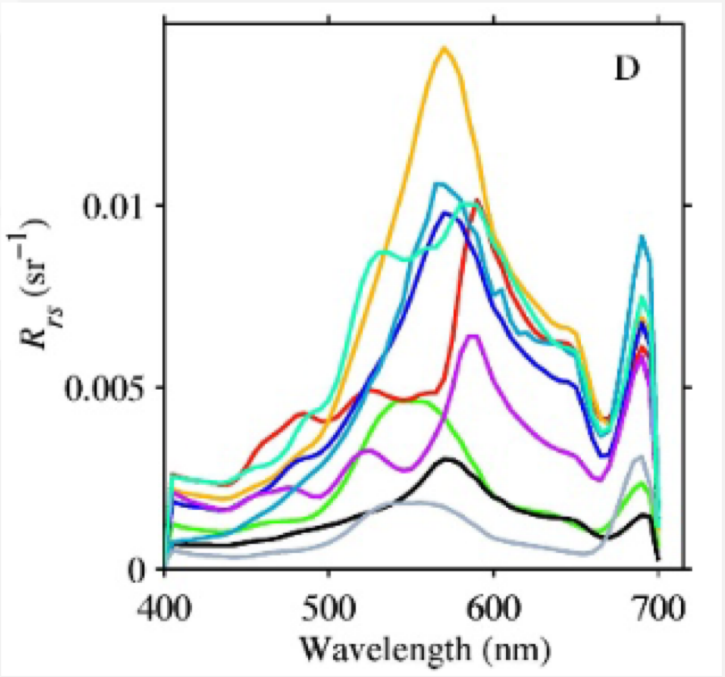
Absorption of individual Pigments



Aph of PFTs



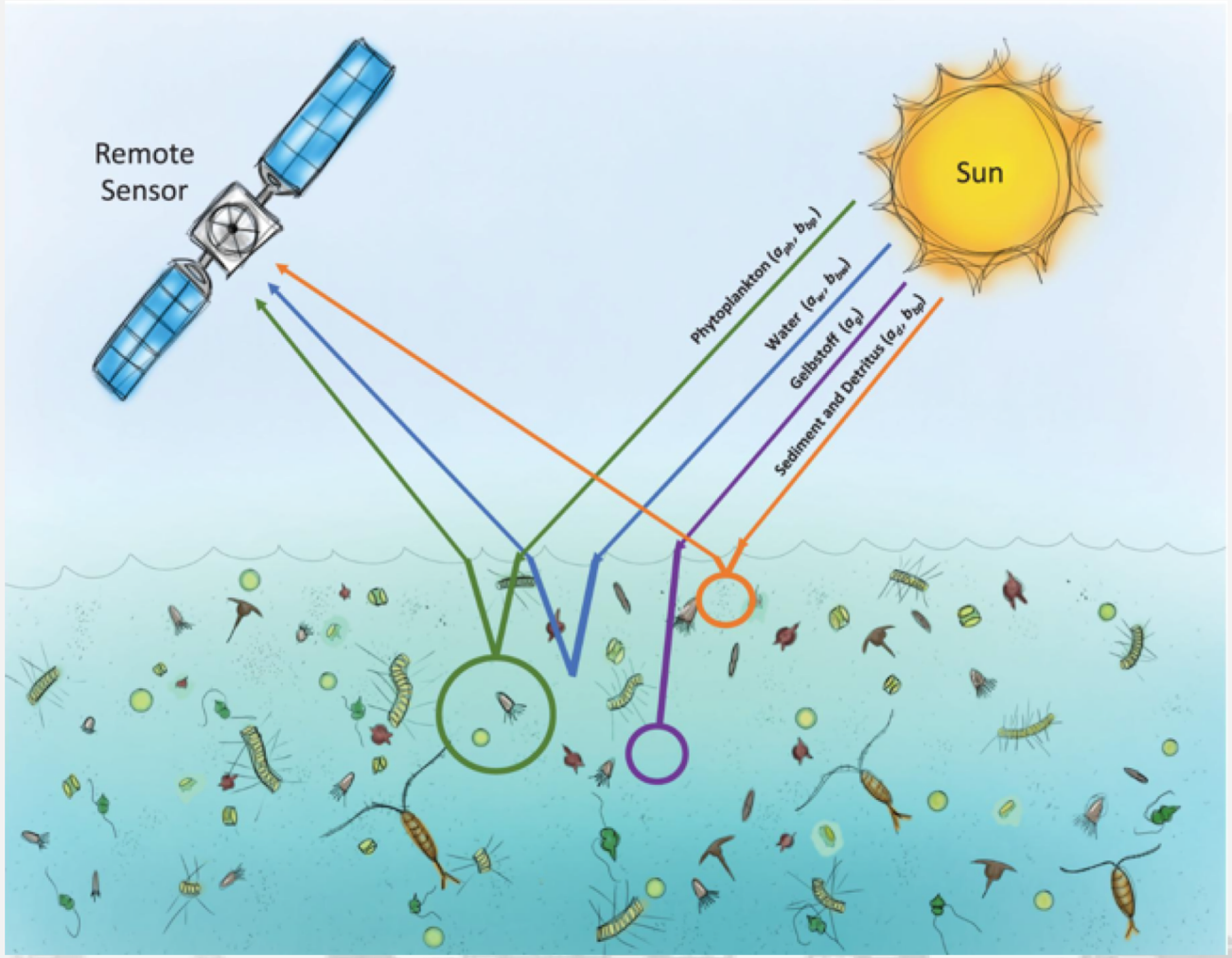
Remote sensing reflectance (Rrs)



(Dierssen et al 2006)

Ocean Color Remote Sensing

How Light Interacts with Water



$$\mathrm{Rrs}(\lambda,0^+) \cong C\,\frac{b_b(\lambda)}{a(\lambda)+b_b(\lambda)}$$

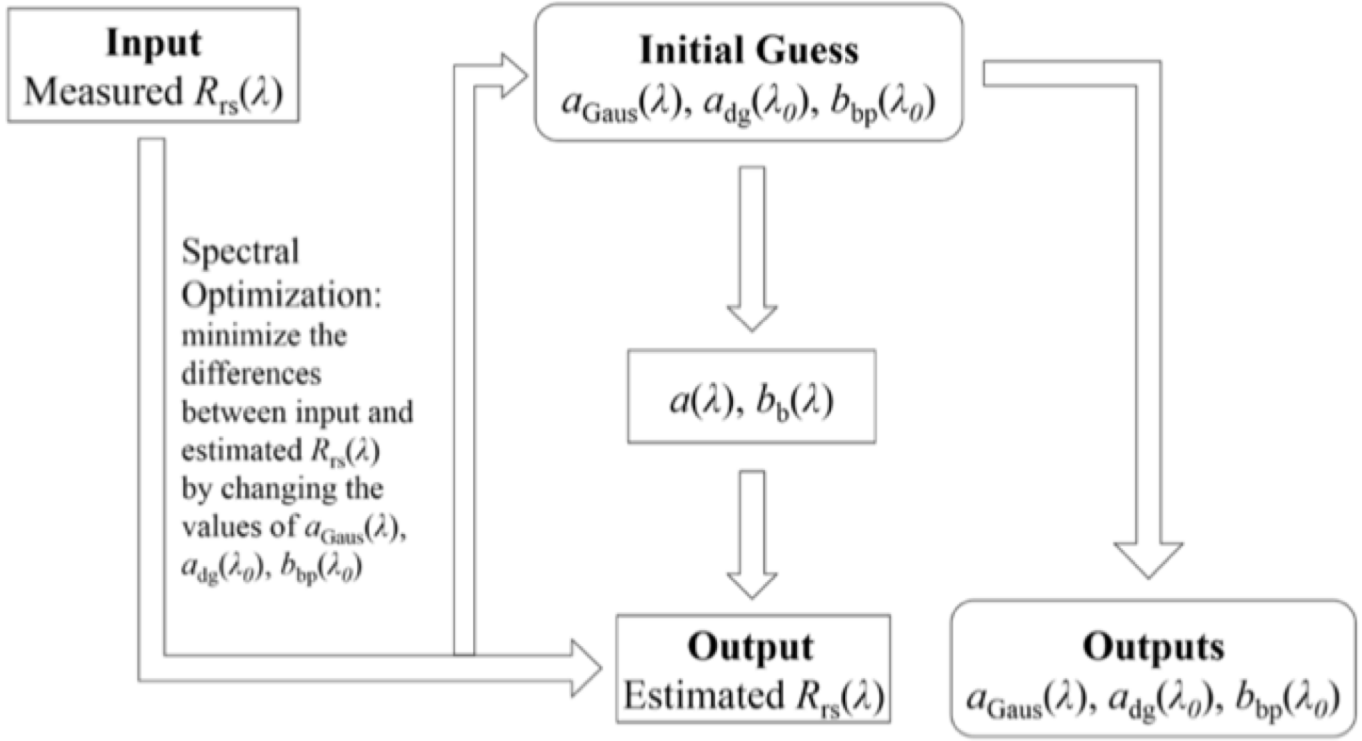
Inherent Optical Properties

a = absorption by…
- phytoplankton (ph)
- non-algal particles (nap)
- colored dissolved organic matter (CDOM)
- water (w)

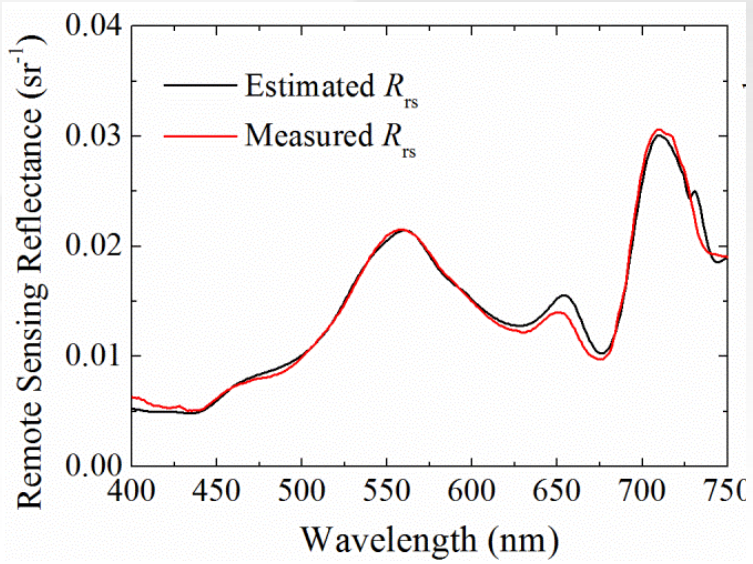
b = scattering in forward (f) and backward (b) directions

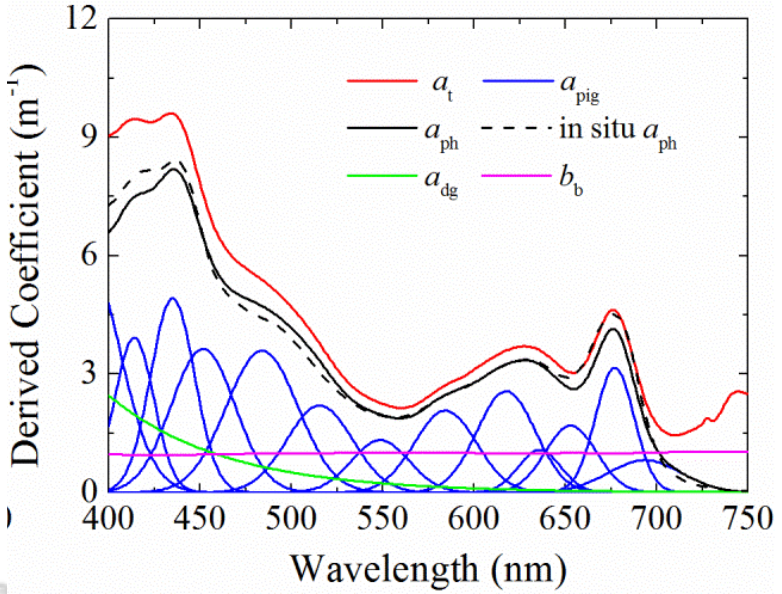
Method

Multi-pigment inversion model (MuPI)



(Wang et al. 2016; Wang, Lee & Mouw, 2017)





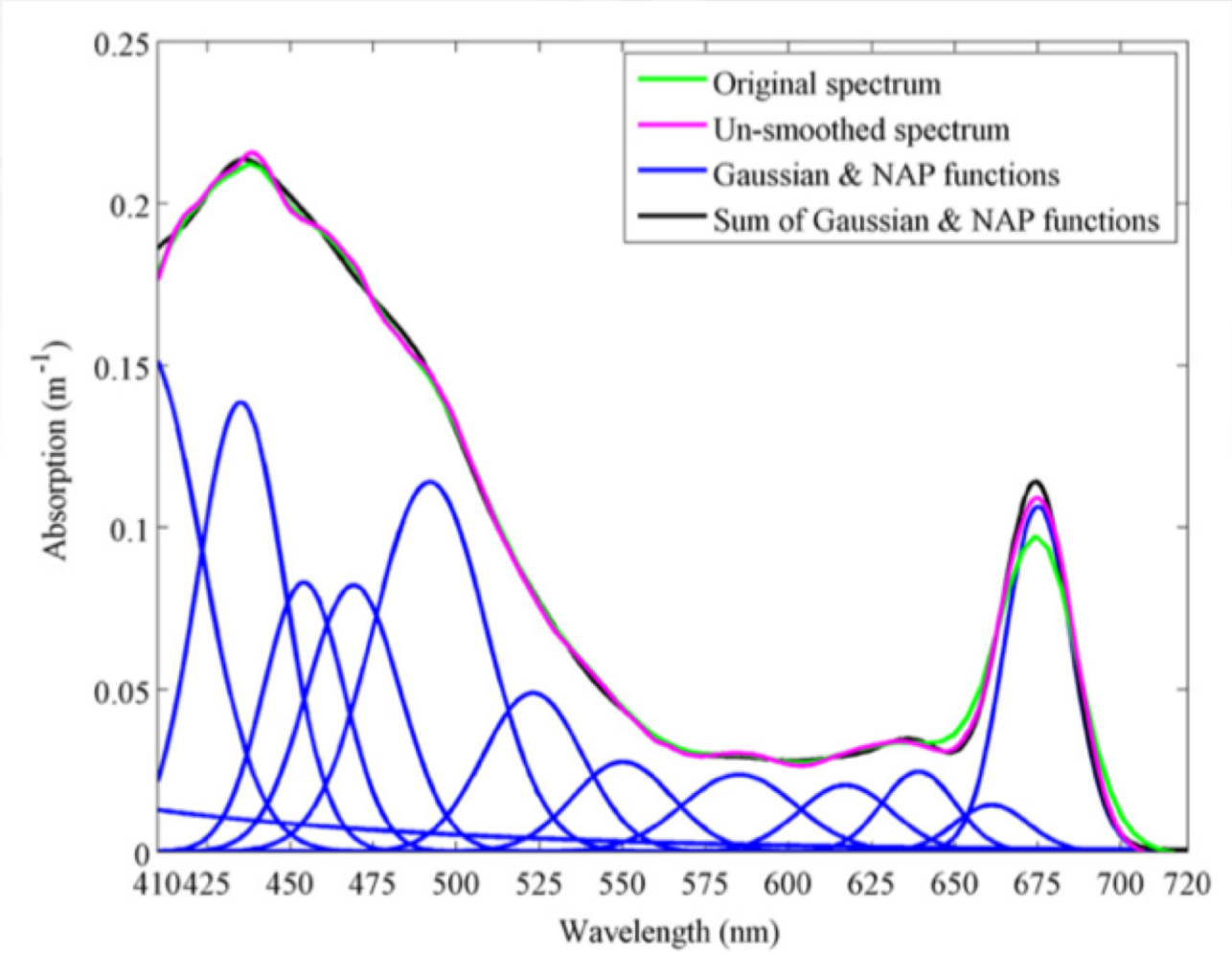
Gaussian decomposition

$$R_{rs}(\lambda)=F\left(\frac{b_b(\lambda)}{a_t(\lambda)+b_b(\lambda)}\right)$$

$$a_{ph}(\lambda)=\sum_{i=1}^{n} a_{gaus}(\lambda_i)\exp\left[-0.5\left(\frac{\lambda-\lambda_i}{\sigma_i}\right)^2\right]$$

$$a_{gau}(\lambda_i) = a_0+a_1 a_{gau}(\lambda_j)$$

$$Cost\ Function = \frac{\sqrt{\frac{1}{n_\lambda}\sum_{\lambda=400}^{\lambda=700}\left(R_{rs}(\lambda)-\hat{R}_{rs}(\lambda)\right)^2}}{\frac{1}{n_\lambda}\sum_{\lambda=400}^{\lambda=700}R_{rs}(\lambda)}$$



Spectrum Optimization

Use QAA-v6 values as first guess of unknown input.

- Sadg : slope of non-algal particle & CDOM absorption (nm-1)
- Adg(443): magnitude of non-algal particle & CDOM absorption (m-1)
- Bbp(443): magnitude of particulate backscattering at 443 nm (m-1)
- m_gaus: magnitude of Gaussian functions representing pigment absorption (m-1)

$$Rrs = f\,(a(\lambda), bb(\lambda))$$

$$a(\lambda) = a_w(\lambda) + a_{ph}(\lambda) + a_y(\lambda) + a_d(\lambda)$$

$$b_b(\lambda) = b_{bw}(\lambda) + b_{b_ph}(\lambda) + b_{b_dm}(\lambda)$$

$$a_y(\lambda) = a_y(440)\,e^{-S_y(\lambda-440)}; \qquad a_y(440) = p_1 \times a_{ph}(440)$$

$$a_d(\lambda) = a_d(440)\,e^{-S_d(\lambda-440)}; \qquad a_d(440) = p_2 \times a_{ph}(440)$$

$$b_{b_ph}(\lambda) = 0.01 \times \left(c_{ph}(\lambda) - a_{ph}(\lambda)\right) \qquad c_{ph}(\lambda) = p_3 \times a_{ph}(440) \times \left(\frac{440}{\lambda}\right)^{p_4}$$

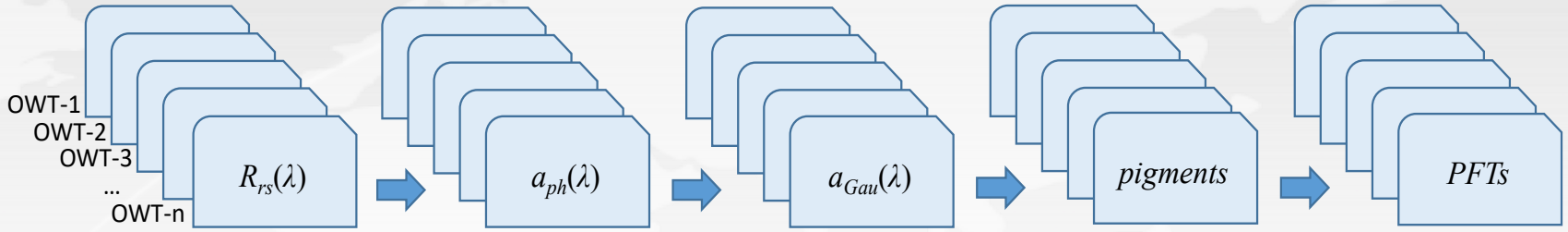
$$b_{b_dm}(\lambda) = p_5 \times a_{ph}(440) \times \left(\frac{440}{\lambda}\right)^{p_6}$$

Update of the Quasi-Analytical Algorithm (QAA_v6)

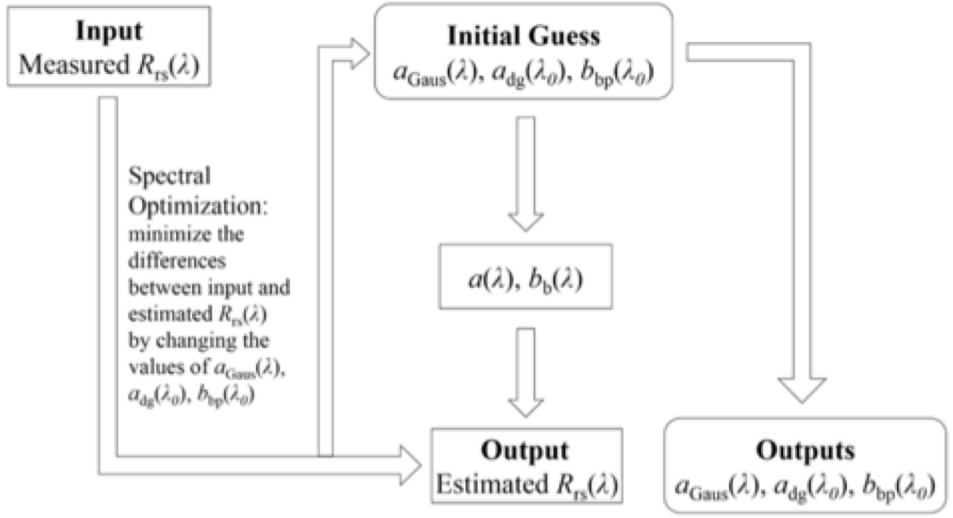
	$r_{rs}(\lambda) = R_{rs}(\lambda)/(0.52 + 1.7\,R_{rs}(\lambda))$	
	$u(\lambda) = \frac{-g_0 + \sqrt{(g_0)^2 + 4g_1 * r_{rs}(\lambda)}}{2g_1}$, where g_0=0.089 and g_1=0.1245	
	IF $R_{rs}(670) < 0.0015\ sr^{-1}$ (QAA_v5)	**(else)**
2	$\chi = \log\left(\frac{r_{rs}(443)+r_{rs}(490)}{r_{rs}(55x)+5\frac{r_{rs}(670)}{r_{rs}(490)}r_{rs}(670)}\right)$ $a(\lambda_0) = a(55x) = a_w(\lambda_0) + 10^{h0+h1\chi+h2\chi^2}$	$a(\lambda_0) = a(670)$ $= a_w(670) + 0.39\left(\frac{Rrs(670)}{Rrs(443)+Rrs(490)}\right)^{1.14}$
3	$b_{bp}(\lambda_0) = b_{bp}(55x) = \frac{u(\lambda_0)\times a(\lambda_0)}{1-u(\lambda_0)} - b_{bw}(55x)$	$b_{bp}(\lambda_0) = b_{bp}(670) = \frac{u(\lambda_0)\times a(\lambda_0)}{1-u(\lambda_0)} - b_{bw}(670)$
4	$\eta = 2.0\left(1 - 1.2\,\exp\left(-0.9\frac{r_{rs}(443)}{r_{rs}(55x)}\right)\right)$	
5	$b_{bp}(\lambda) = b_{bp}(\lambda_0)\left(\frac{\lambda_0}{\lambda}\right)^{\eta}$	
6	$a(\lambda) = (1-u(\lambda))(b_{bw}(\lambda) + b_{bp}(\lambda))/u(\lambda)$	
7 & 8	$\zeta = 0.74 + \frac{0.2}{0.8 + r_{rs}(443)/r_{rs}(55x)}$ $\xi = e^{S(442.5-415.5)}, S = 0.015 + \frac{0.002}{0.6 + r_{rs}(443)/r_{rs}(55x)}$	
9 & 10	$a_g(443) = \frac{a(412)-\zeta a(443)}{\xi-\zeta} - \frac{a_w(412)-\zeta a_w(443)}{\xi-\zeta}$ $a_{dg}(\lambda) = a_g(443)e^{-S(\lambda-443)}$, $a_{ph}(\lambda) = a(\lambda) - a_{dg}(\lambda) - a_w(443)$	

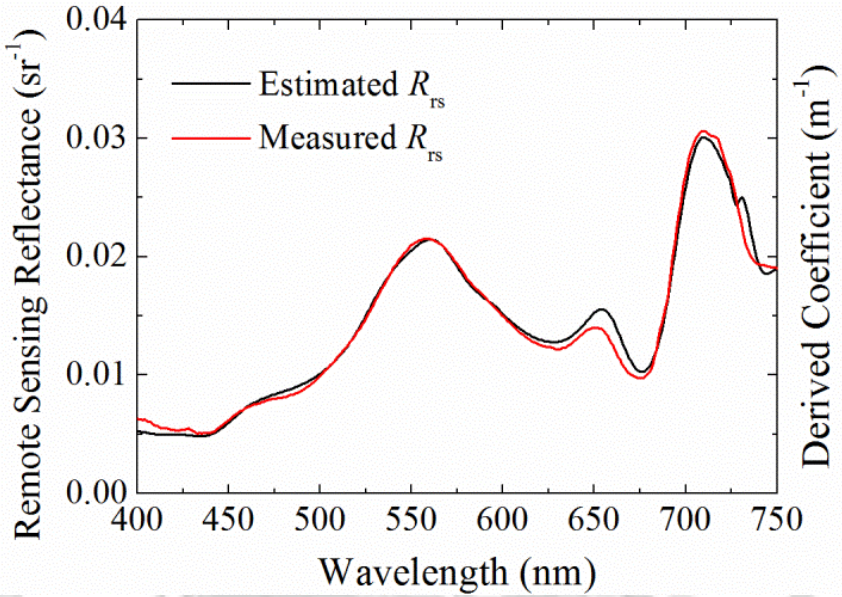
Method

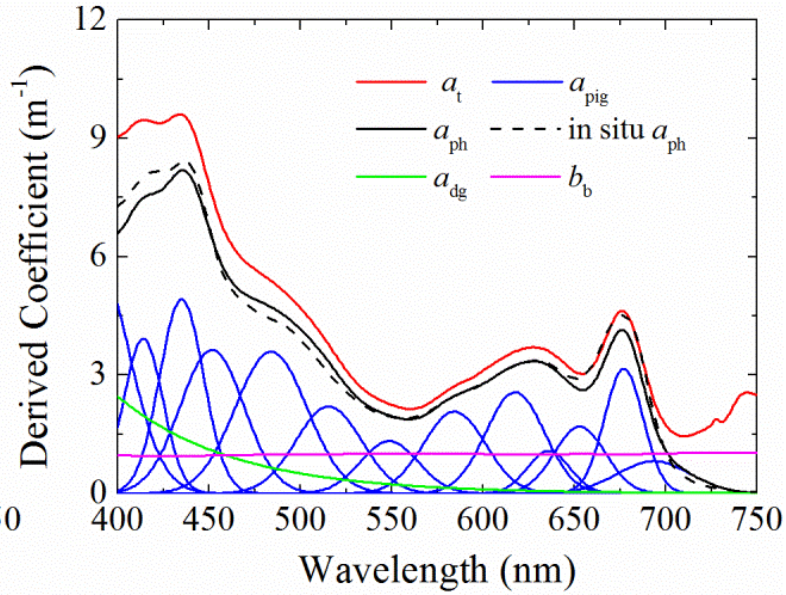
Multi-pigment inversion model (MuPI)



$$R_{rs}(\lambda) = f\left(\frac{b_b}{a_t + b_b}\right) = f\left(\frac{b_{bw} + 0.01\left(c_s - a_{ph}(\lambda)\right)}{\sum_{i=1}^{n} a_{gaus}(\lambda_i)\exp\left[-0.5\left(\frac{\lambda - \lambda_i}{\sigma_i}\right)^2\right] + a_{dg}(\lambda_0)\exp\left(-S(\lambda - \lambda_0)\right) + a_w + b_{bw} + 0.01\left(c_s - a_{ph}(\lambda)\right)}\right)$$







Case 1: Application to coastal area

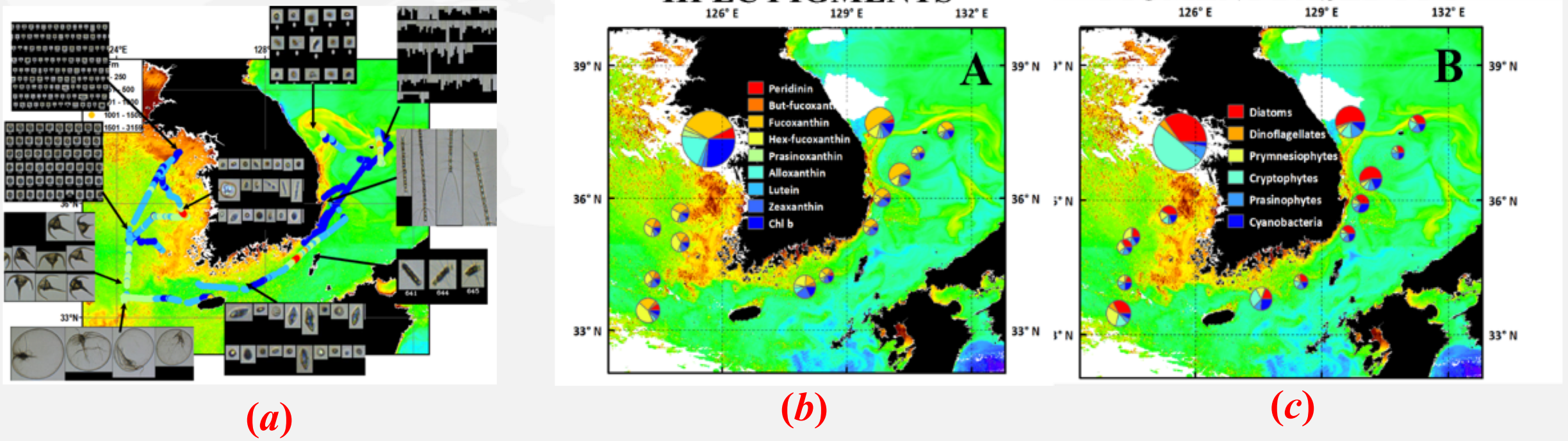


Fig. (*a*) Phytoplankton species distribution, (b) Pigment compositions (%) by HPLC (c) PFTs obtained by CHEMTAX analysis of HPLC pigments

(Wu et al 2022, RSE)

Case 1: Application to coastal area

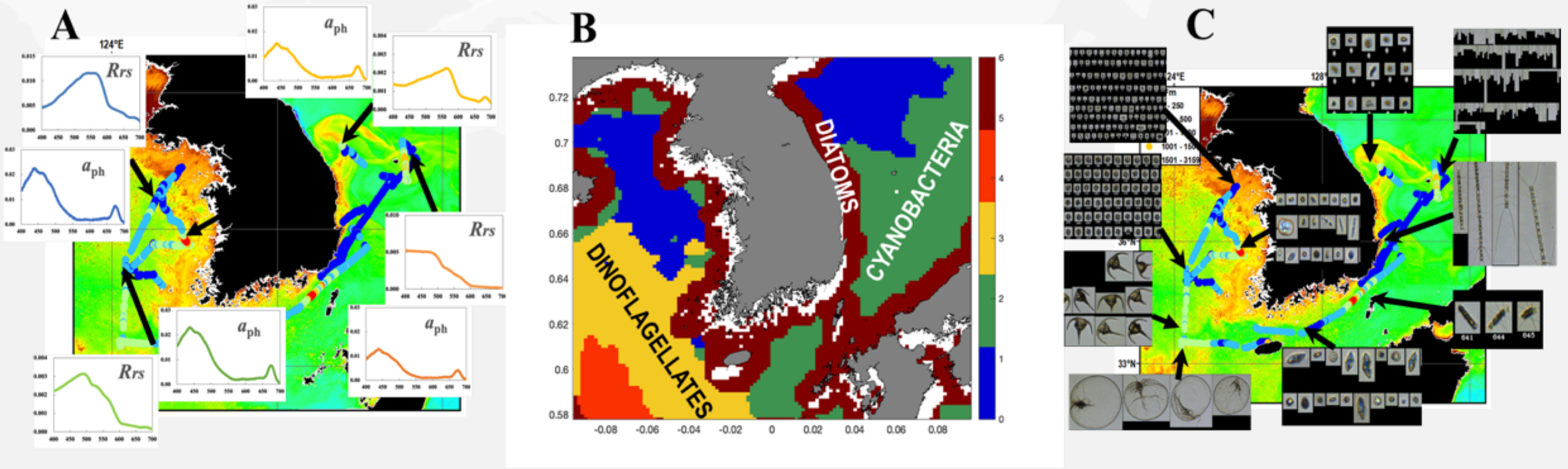
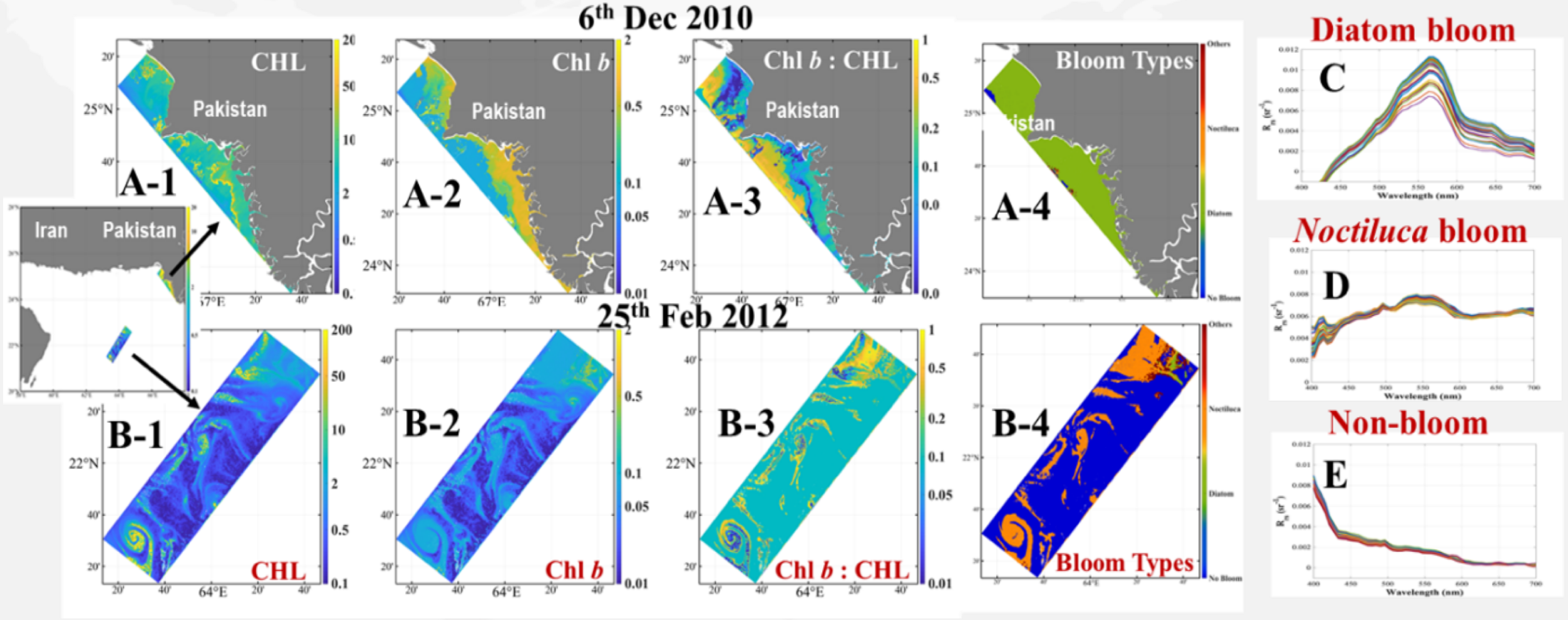


Figure. (A) differences in in-situ $R_{rs}(\lambda)$ and $a_{ph}(\lambda)$ obtained during the NASA KORUS cruise (May-June 2016). (B) O-BGC Biomes generated using GOCI, plus hydrographic and bathymetry data. (C) Phytoplankton functional types obtained with the help of a FlowCAM operated using a continuous flow-through system developed by co-I Goes.

(Wu et al 2022, RSE)

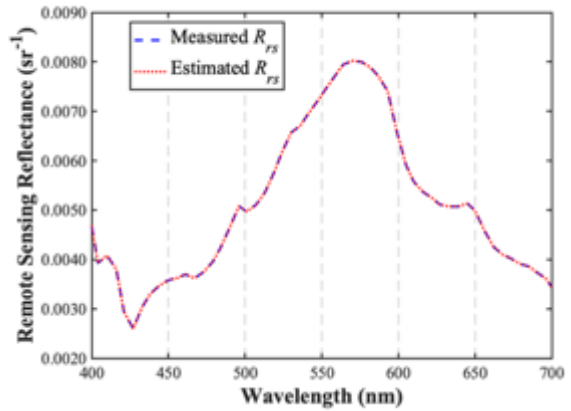
Case 2: Application to AVIRIS-NG and PRISM overflights

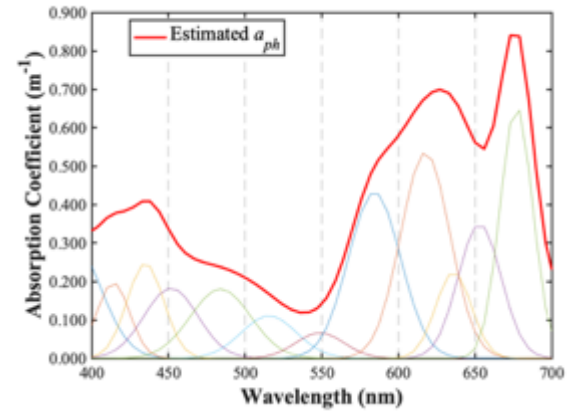


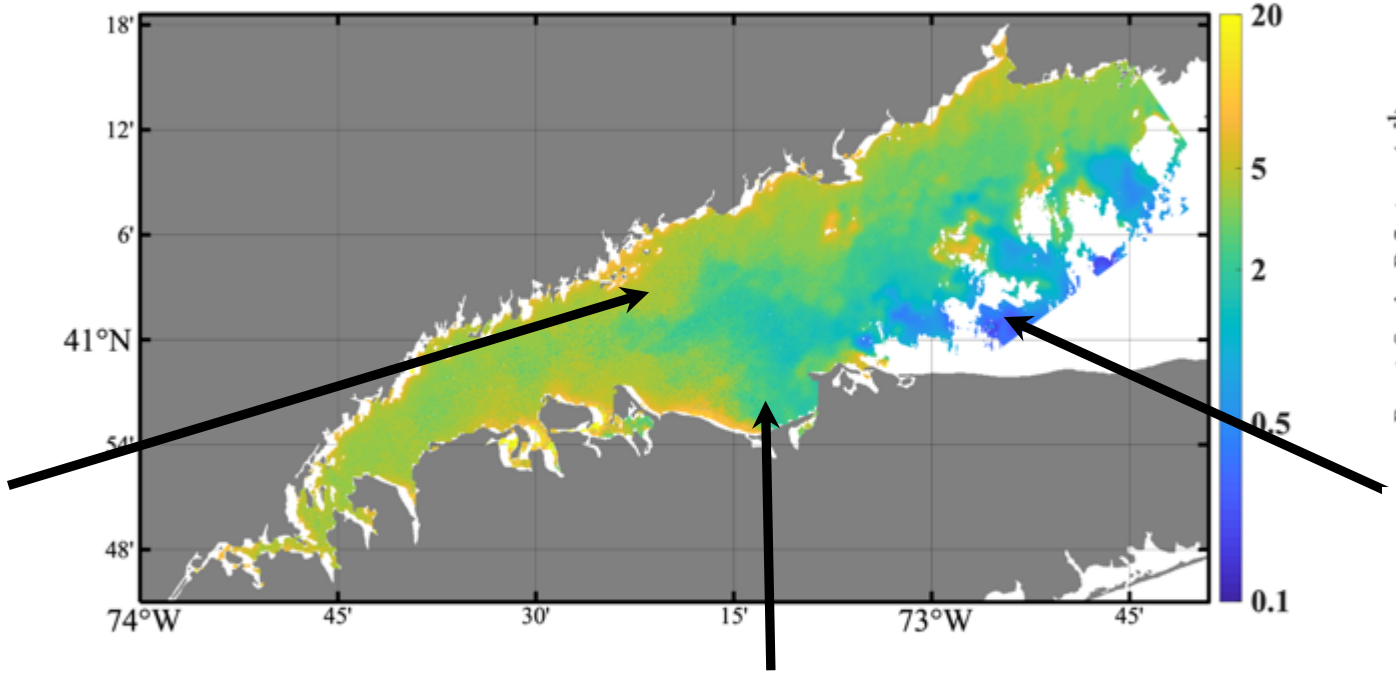
Chlb/Chla ratio ≥ 0.25 Noctiluca; Chlb/Chla ratio < 0.25 Diatoms

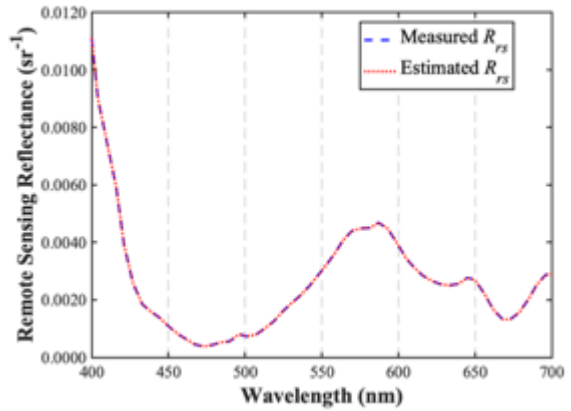
Case 3: Apply to HICO images – Long Island Sound

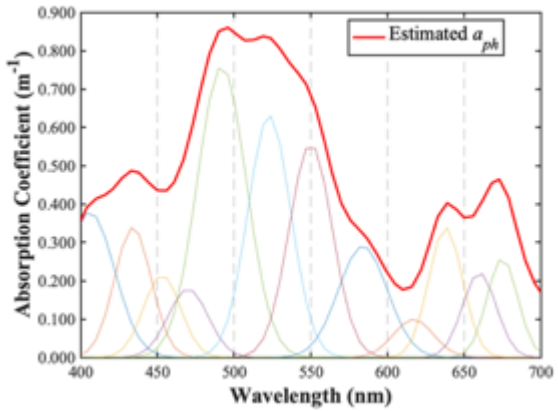
Hyperspectral $R_{rs}(\lambda)$, $a_{ph}(\lambda)$, and MuPI derived Gaussian pigment peaks for phytoplankton derived for locations in LIS using HICO image for 18th Jan 2010. Figures shows comparisons of $R_{rs}(\lambda)$ and $a_{ph}(\lambda)$ derived from HICO with in-situ $R_{rs}(\lambda)$ and $a_{ph}(\lambda)$measured at arrow locations on same day at LISCO Observatory (Sami and Gilerson, CCNY) .

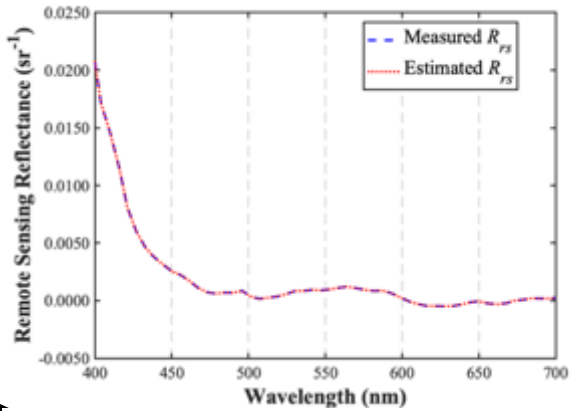


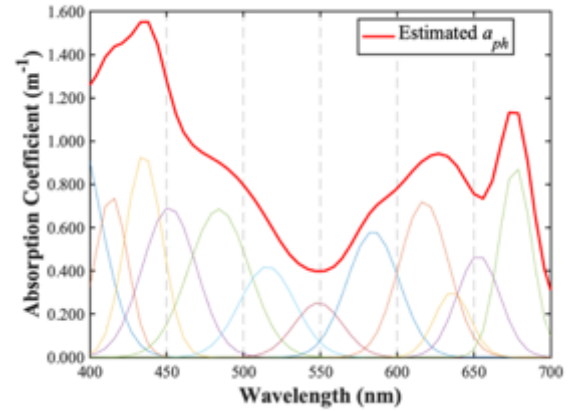






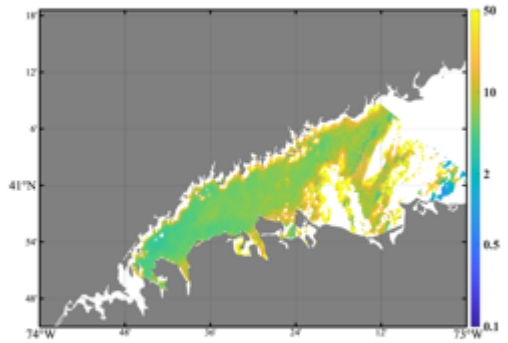




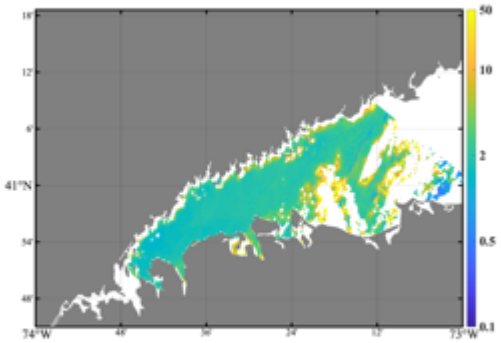


Case 3: Apply to HICO images – Long Island Sound

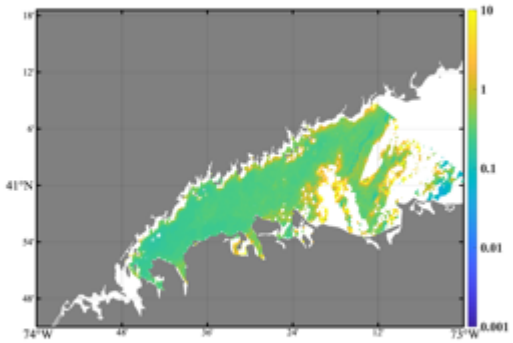
Pigment fields derived from LIS HICO image of 18th Jan 2010 using MuPI



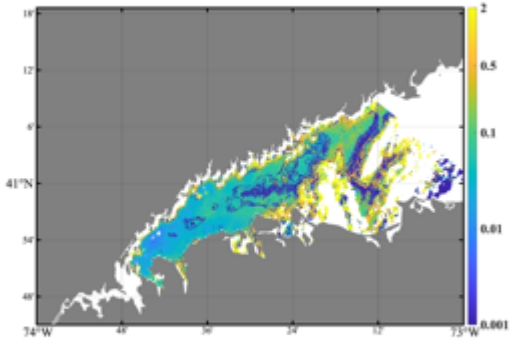
CHL-HICO



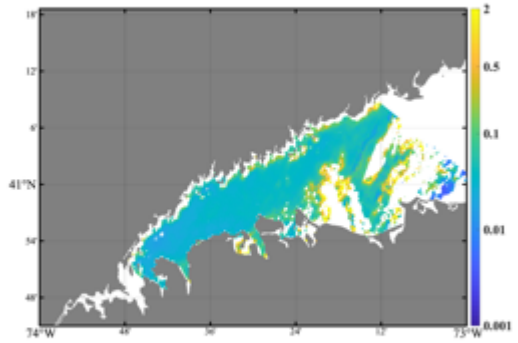
Chl *a*



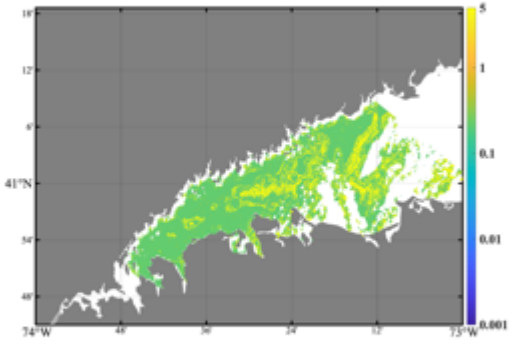
Chl *b*



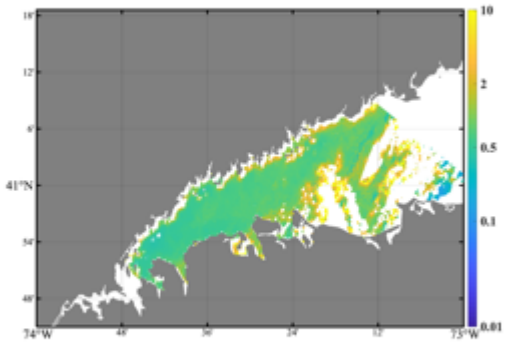
Chl *c*



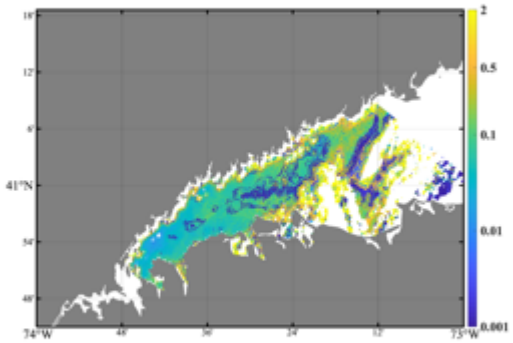
PC



PE



PPC

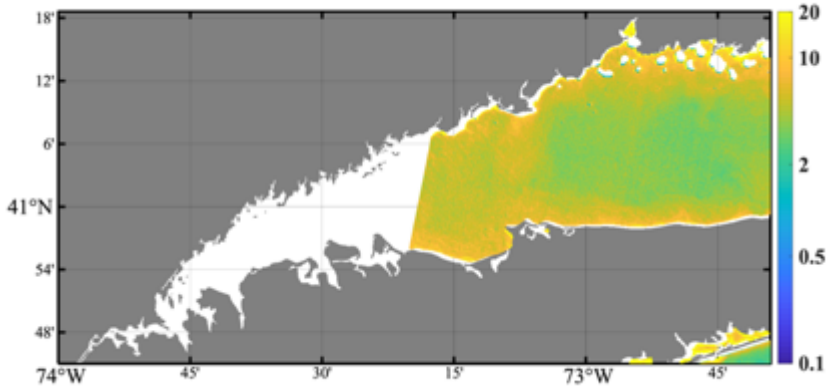


PSC

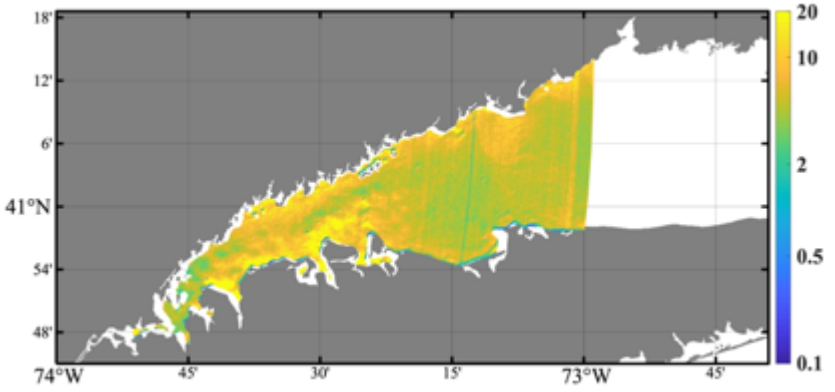
PE-phycoerythrin related to the concentration of M. rubrum cells

MuPI model could also applied on Hawkeye images

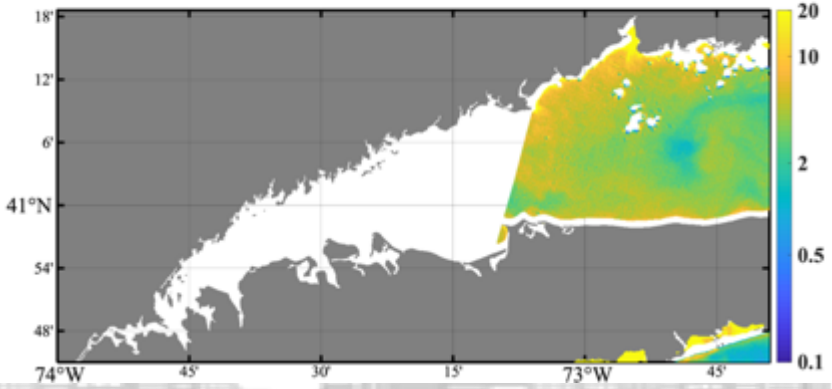
Hawkeye - CHL



CHL - 2021/05/12



CHL – 2021/05/14



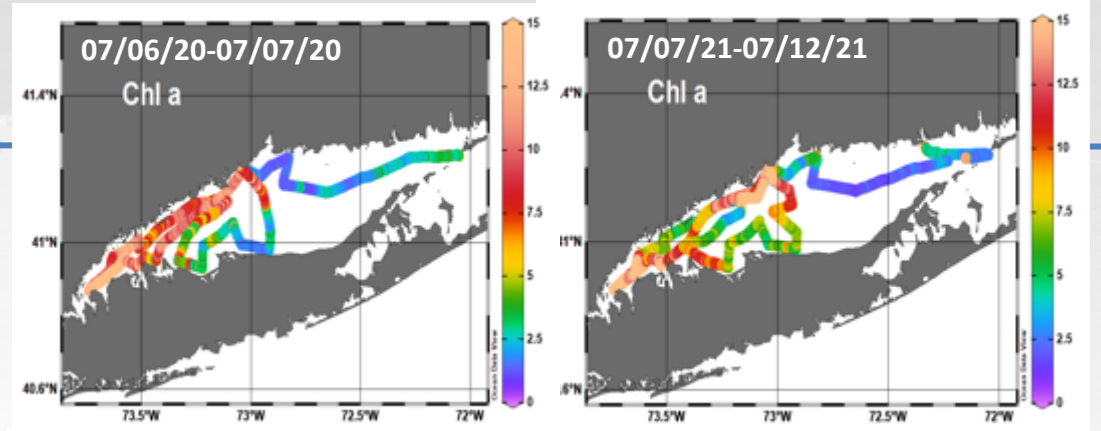
CHL – 2021/07/30

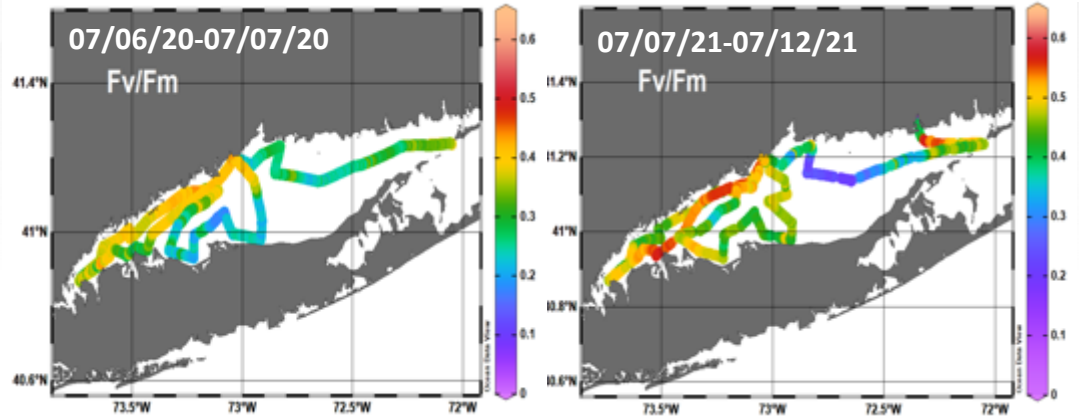
6-7th July 2020 *Prorocentrum* micans)

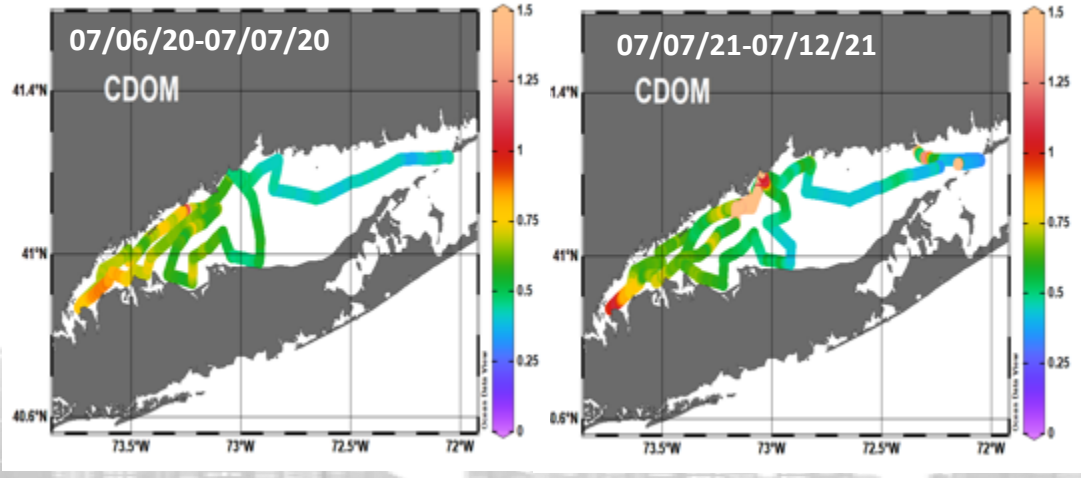




7-12th July 2021 Diatoms







Thank you for your attention!

Phytoplankton Function Types (PFTs)

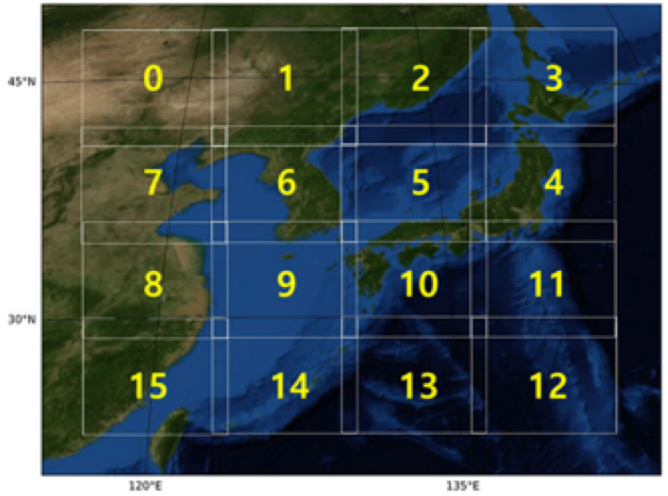
Mosaic of morphological traits in phytoplankton.

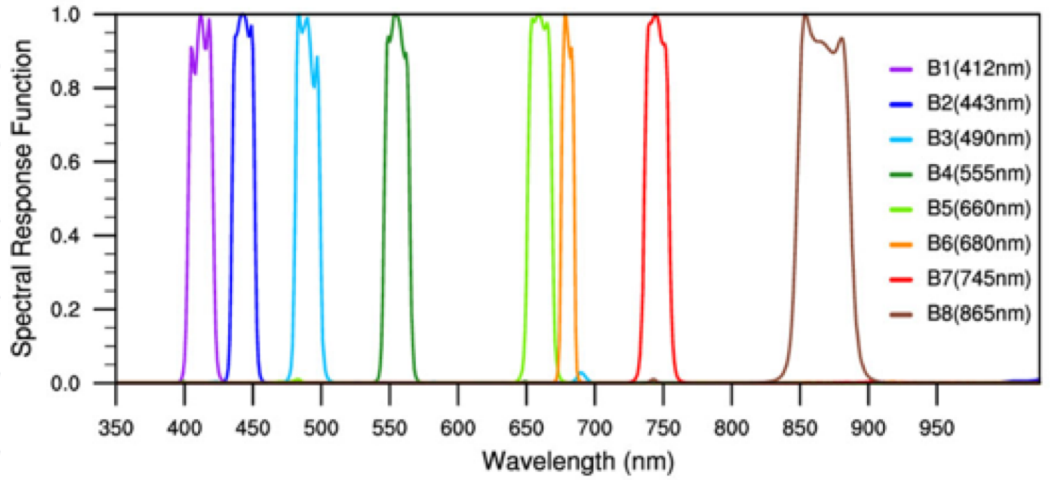
(A) One-dimensional chain of the dinoflagellate Alexandrium catenella.
(B) Solitary cell of the dinoflagellate Alexandrium catenella.
(C) One-dimensional chain of the diatom Chaetoceros convolutes with hollow spines containing chloroplasts.
(D) Scanning electron-microscopy (SEM) image of phytoplankton natural assemblage from the North Sea (Bergen, Norway), including Skeletonema sp., Pseudo-nitzschia sp., and various coccolithophorids.
(E) Motile solitary cells of the prymnesiophyte Phaeocystis globosa.
(F) Three-dimensional non-motile colonial structure of the prymnesiophyte Phaeocystis globosa.
(G) One-dimensional chain of the diatom Thalassiosira rotula.
(H) SEM image of the cosmopolitan coccolithophore Emiliania huxleyi, whose cell wall plates (liths) are made of calcium carbonate.
(I) Spiny solitary cells (top) and a one-dimensional chain (bottom) of the green alga Scenedesmus quadricauda.
(J) One-dimensional chains (four cells) and a two-dimensional plate (eight cells) of the green alga Scenedesmus obliquus.
(K) A large cell of the dinoflagellate Ceratium trichoceros.
(L) SEM image of the dinoflagellate Phalacroma sp. with a cellulosic cell wall (left), and the diatom Thalassiosira sp., whose cell wall (frustule) is made of silica (right).
(M) One-dimensional chain of the diatom Dactyliosolen fragilissimus with short and straight marginal spines.



Geostationary Ocean Color Imager (GOCI)

Item	Geostationary Ocean Color Imager (GOCI)
Development/Operation	This satellite was developed by the Korea Aerospace Research Institute and the ASTRIUM (present AIRBUS), a French company, and mainly operated by the Korea Ocean Satellite Center of the Korea Institute of Ocean Science & Technology
Launching Date	2010-06-27
Orbit	Altitude 35,786 km, 128.2°E
Performance Period	Aug. 2010 — Mar. 2011 (initial test operation) Apr. 2011 — Mar. 2018 (7 years for regular mission) 1st extension: Apr. 2018 — Mar. 2020 2nd extension: Apr. 2020 — Mar. 2021
Spatial Resolution	500m
Temporal Resolution	1 hour (8 times/day, 0 UTC — 7 UTC)
Band	8 bands (6 bands for visible light, 2 bands for near-infrared ray)
Spectral Range	412 ~ 865nm
Imaging Area	Regional 2,500 km X 2,500 km (Center coordinate 130°E, 36°N)
Imaging Slot	16 slots (Total 5,685 X 5,567 Pixels)
Products	13 types (Remote sensing reflectance, chlorophyll concentration, total suspended solids concentration, absorption by dissolved organic matter, diffuse attenuation coefficient for downward irradiance, Secchi depth, marine primary productivity, red tide, surface layer current, aerosol optical depth, aerosol type (yellow sand), terrestrial vegetation index, and enhanced vegetation index)





AVIRIS-NG and PRISM



AVIRIS-NG measures the wavelength range from 380 nm to 2510 nm with 5 nm sampling. Spectra are measured as images with 600 cross-track elements and spatial sampling from 0.3 m to 4.0 m from a Twin Otter platform. In the future, a high altitude platform is expected to be available. AVIRIS-NG has better than 95% cross-track spectral uniformity and >= 95% spectral IFOV uniformity.



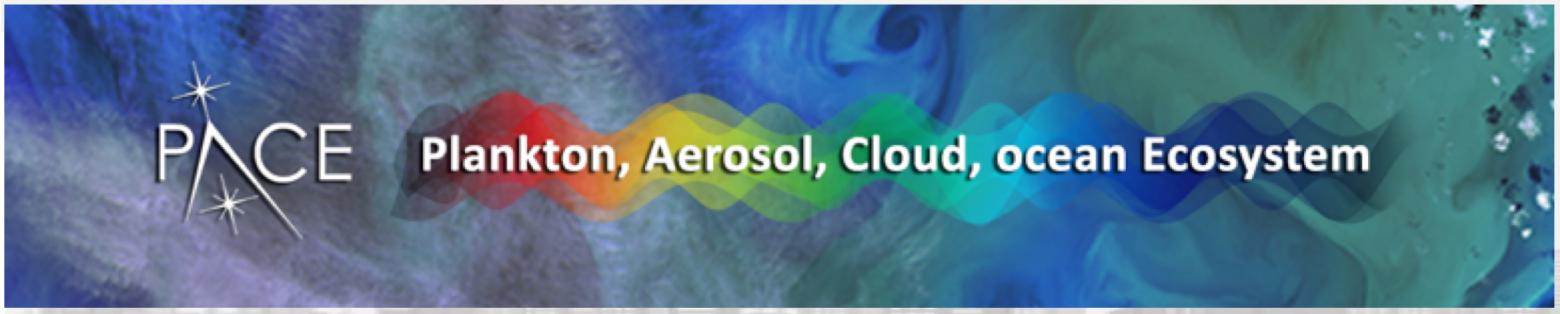
PRISM comprises a pushbroom imaging spectrometer covering the near UV to near IR range (350-1050 nm) and a separate spot radiometer covering two short wave infrared (SWIR) bands at 1240 and 1610 nm respectively.

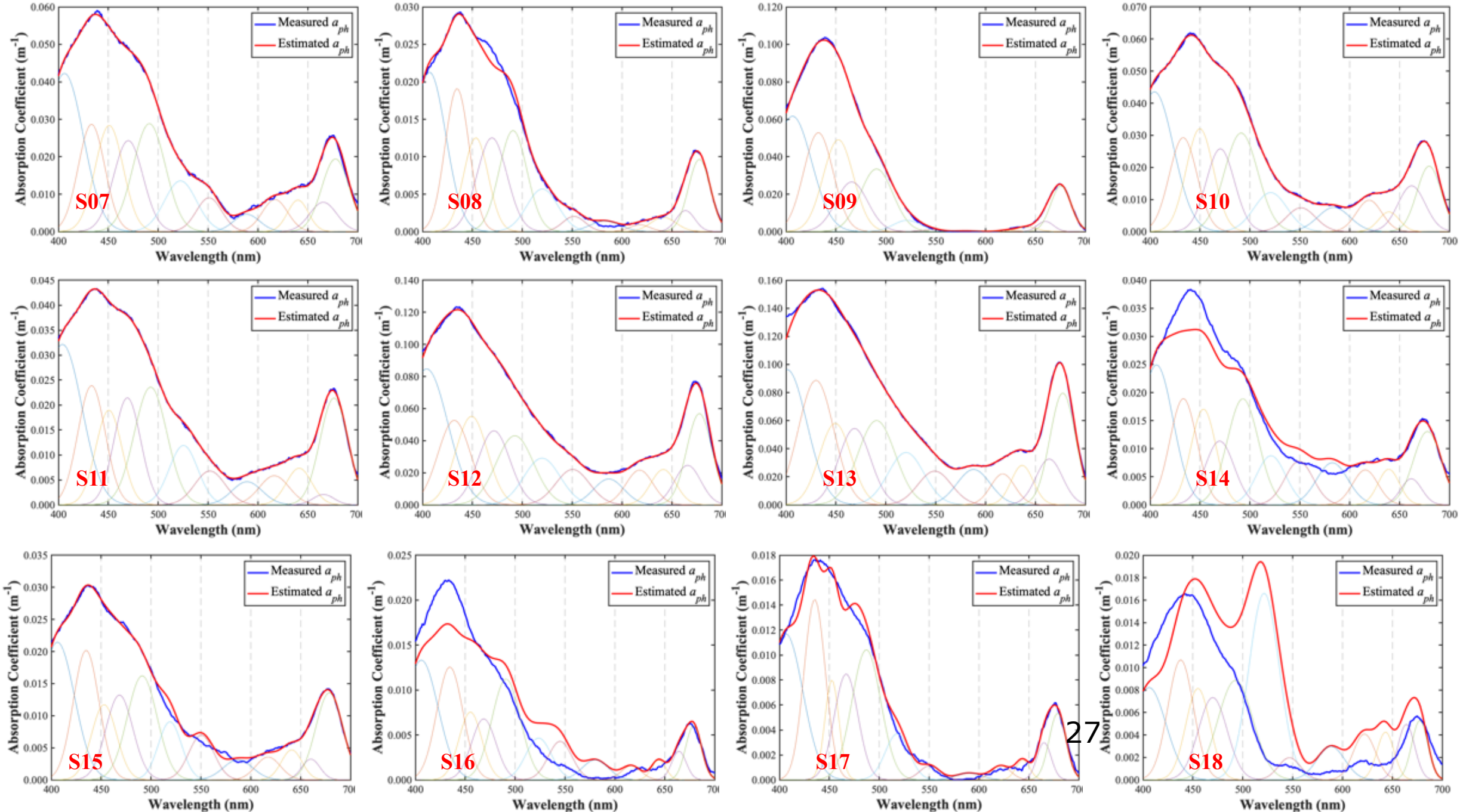
HICO



The Hyperspectral Imager for the Coastal Ocean (HICO™) is an imaging spectrometer based on the PHILLS airborne imaging spectrometers. HICO is the first spaceborne imaging spectrometer designed to sample the coastal ocean. HICO samples selected coastal regions at 90 m with full spectral coverage (380 to 960 nm sampled at 5.7 nm) and a very high signal-to-noise ratio to resolve the complexity of the coastal ocean. As a demonstrative instrument, HICO was designed to collect only one 50 x 200 km scene per orbit. The regions to be collected were determined weekly by a scheduling team. The focus was on providing HICO data for scientific research on coastal zones and other regions around the world. HICO demonstrates coastal products including water clarity, bottom types, bathymetry and on-shore vegetation maps. During its five years in operation HICO collected over 10,000 scenes from around the world.

SPEXone's Journey... Next Stop: PACE




S07
S08
S09
S10
S11
S12
S13
S14
S15
S16
S17
S18
Measured a_{ph}
Estimated a_{ph}
Absorption Coefficient (m^{-1})
Wavelength (nm)

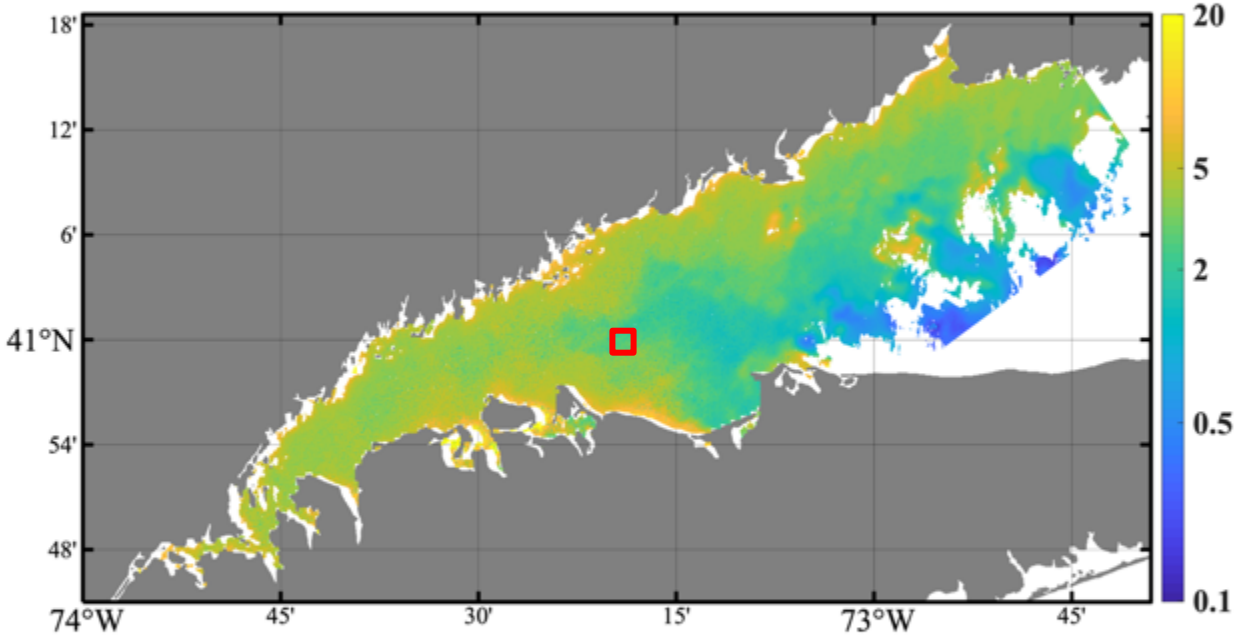
Validation: pigments

		Percentages				Pigment Ratio
Station	Depth (m)	Diatoms	Dinoflagellates (excluding Noctiluca)	Other Algae	Noctiluca	Chlb/Chla
1	0	47.5	20.0	0.0	32.5	0.25
2	0	80.0	15.0	0.0	5.0	0.10
3	0	24.2	7.6	0.0	68.2	0.20
4	0	25.7	7.1	0.0	67.1	0.22
5	0	95.5	4.5	0.0	0.0	0.03
6	0	93.7	5.9	0.5	0.0	0.03
7	0	97.7	2.3	0.0	0.0	0.01
8	0	100.0	0.0	0.0	0.0	0.12
9	0	40.0	10.0	0.0	50.0	0.18
10	0	75.0	18.8	6.3	0.0	0.05
11	0	44.4	55.6	0.0	0.0	0.10
12	0	66.7	33.3	0.0	0.0	0.09
13	0	33.3	66.7	0.0	0.0	0.10

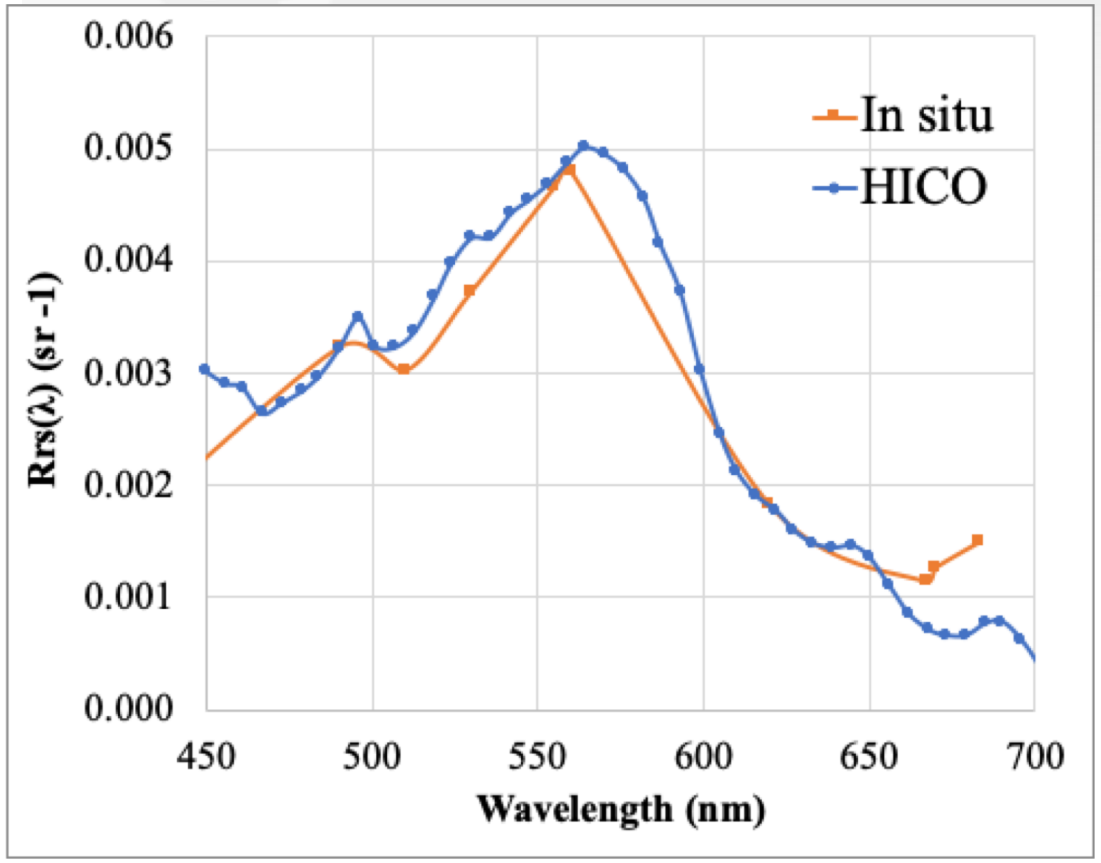
HPLC data and taxonomy from 2011 cruise

Validation

2010/018



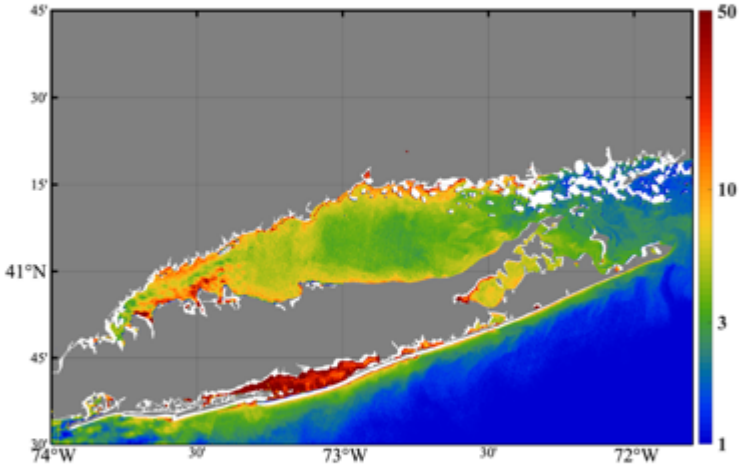
Lon = -73.34 Lat = 40.95



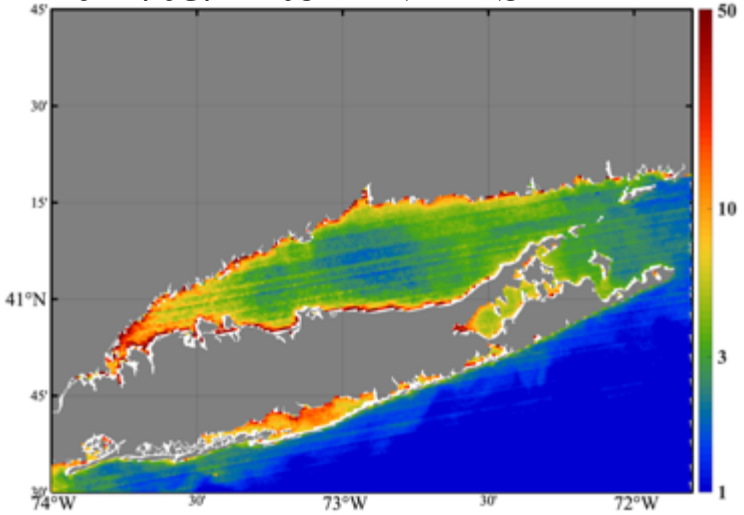
In situ Rrs from aoc_LISCO cruise, contributed by Sam_Ahmed_and_Alex_Gilerson

Different season: May & July 2021

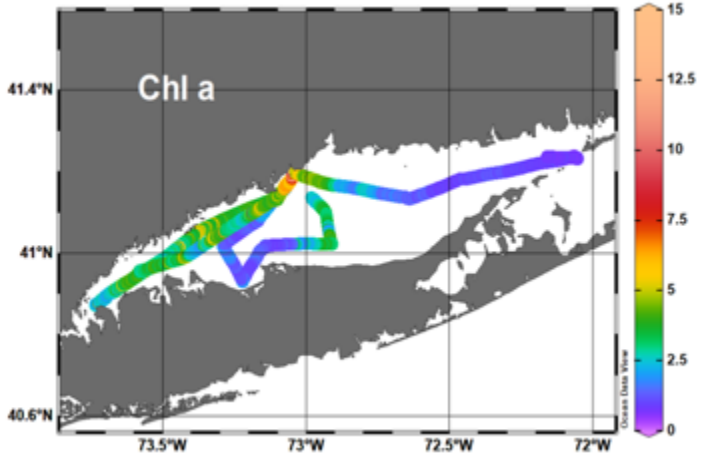
2021/05/12 to 14 Hawkeye



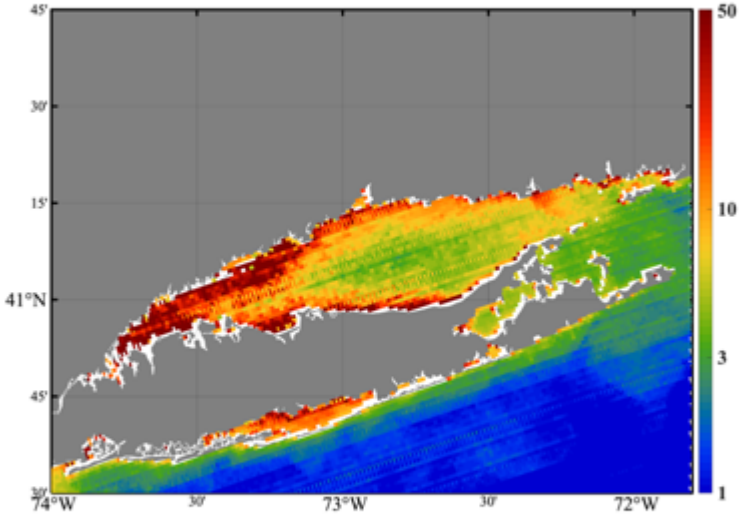
2021/05/12 to 14 VIIRS

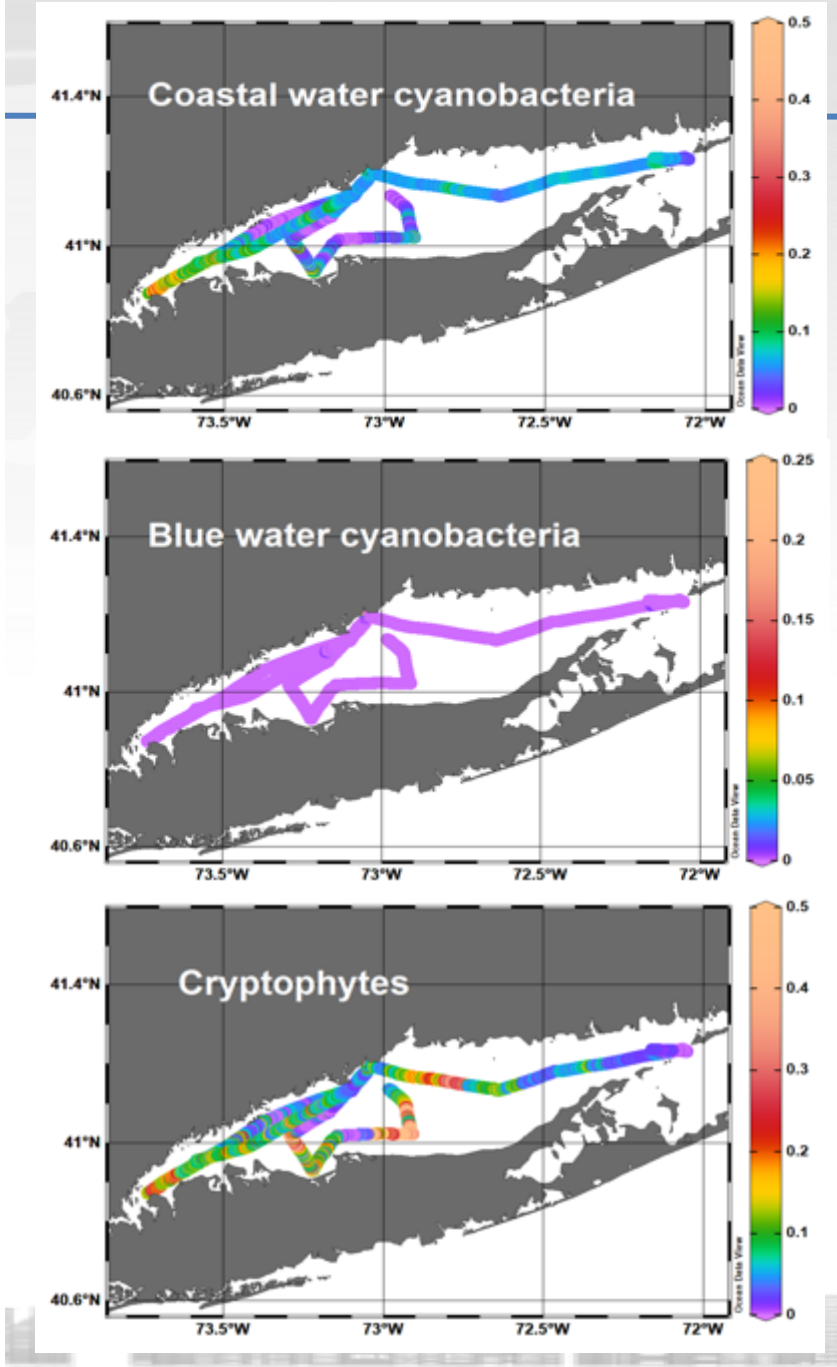


2021/05/04 to 06 *in situ*

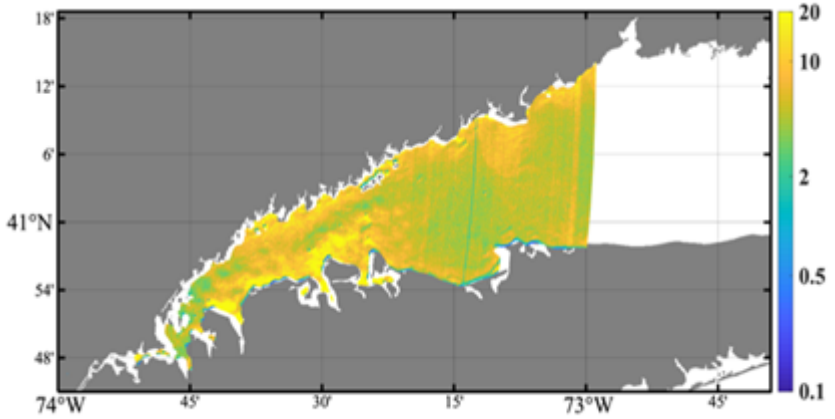


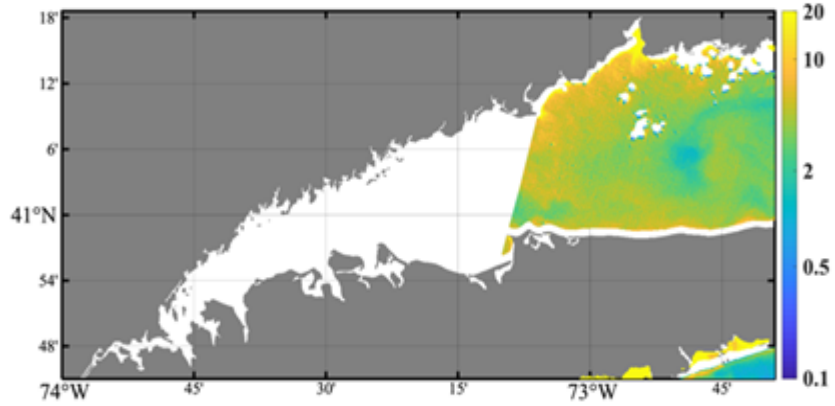
2021/05/04 to 06 VIIRS



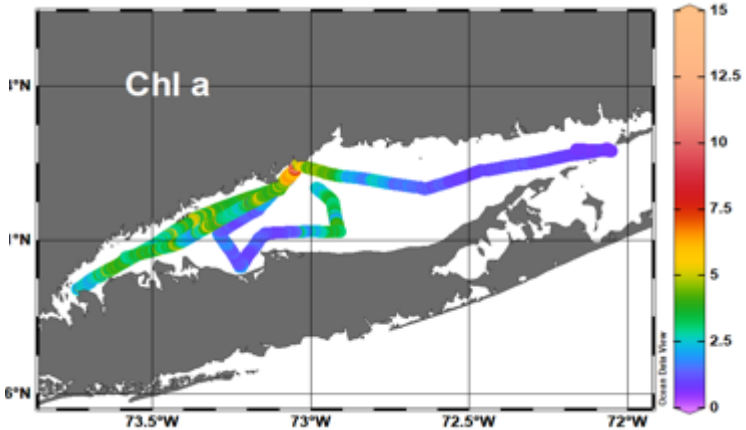


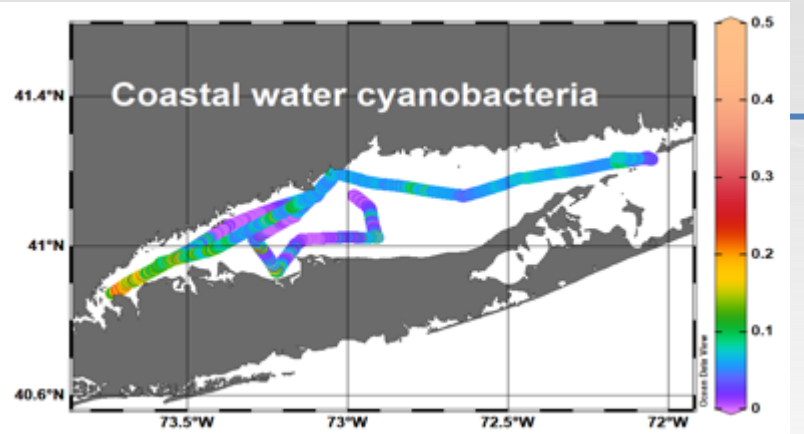
2021/05/14

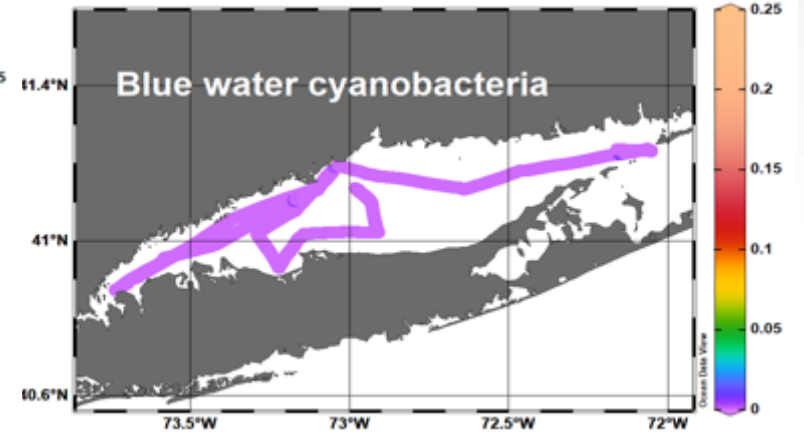


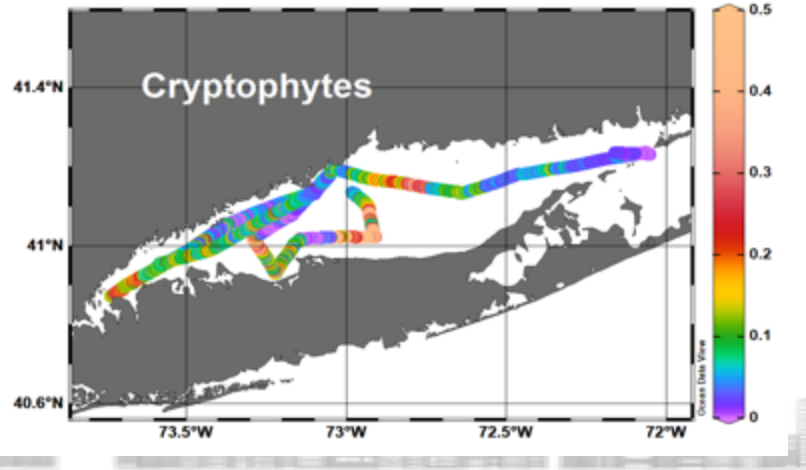


2021/05/04 to 06



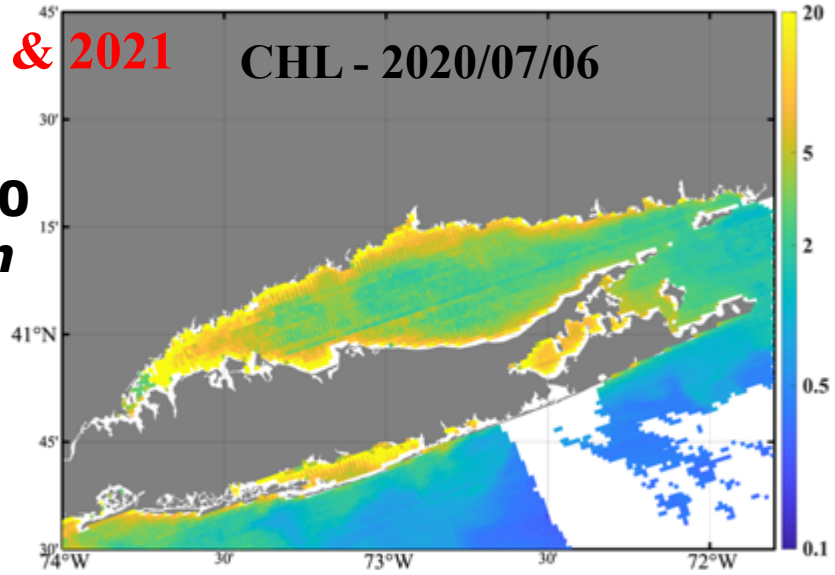


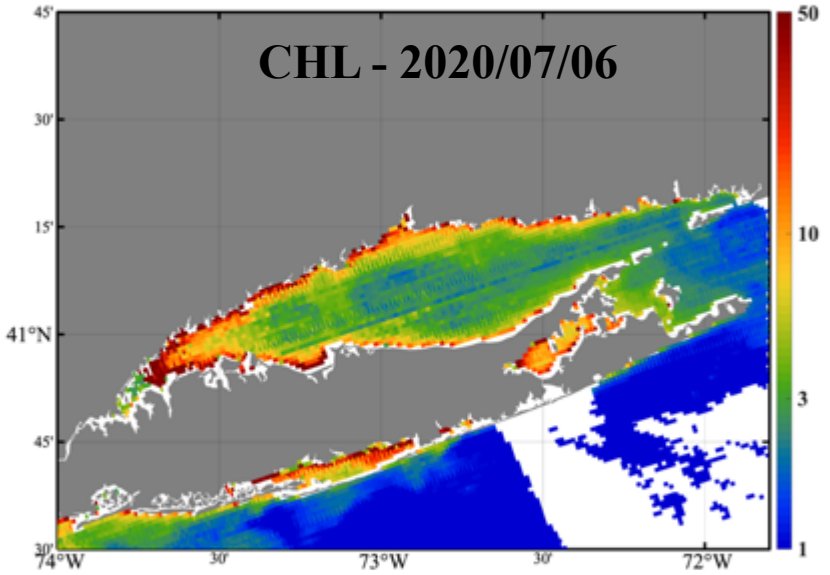




July 2020 & 2021

6-7th July 2020
Prorocentrum

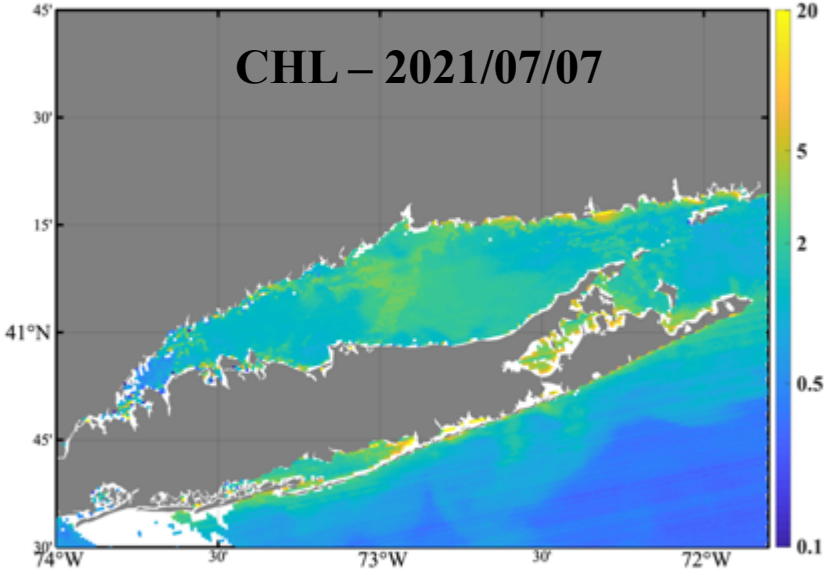


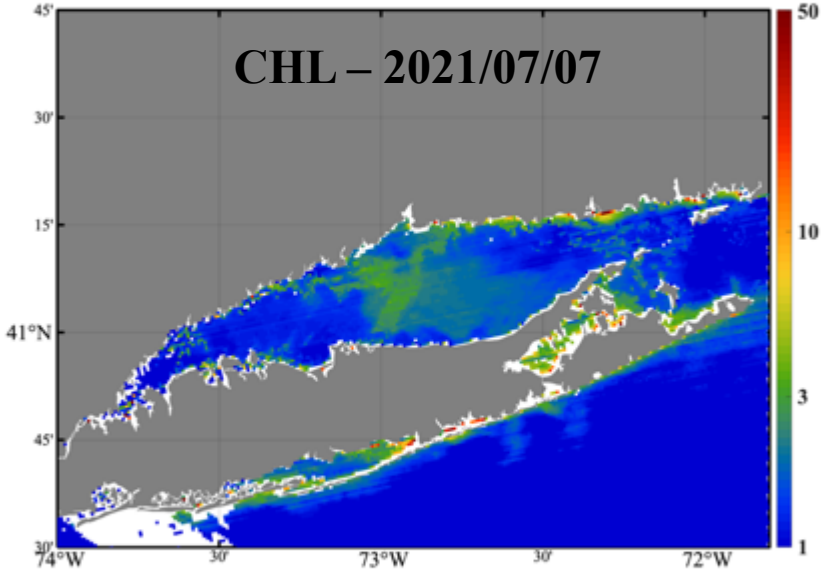


VIIRS

The left and right figures show same data with different colorbar

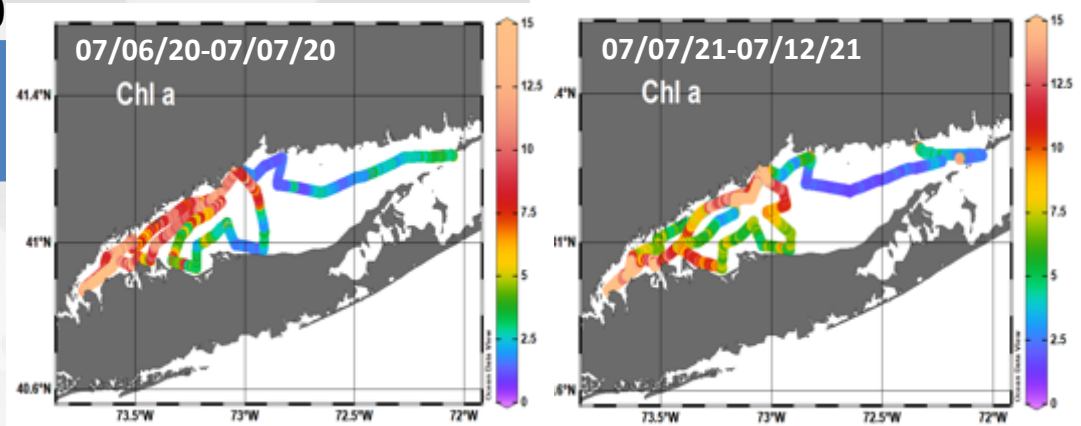
7-12th July 2021
Diatoms

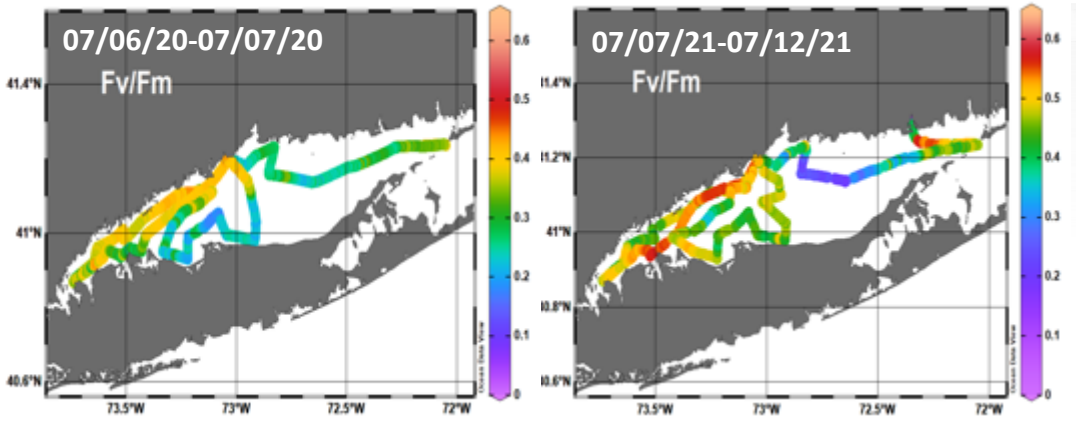


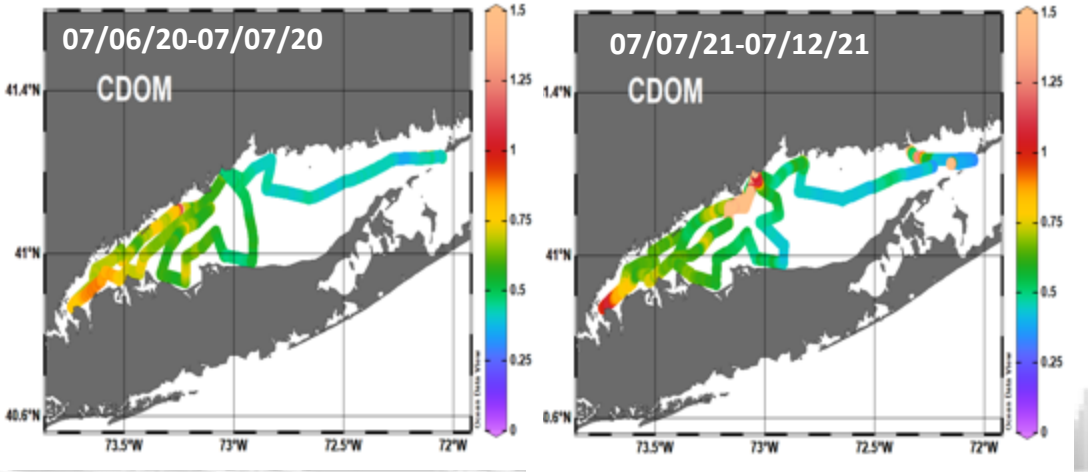


-7th July 2020

Prorocentrum







7-12th July 2021 Diatoms

VIIRS

